I give permission for public access to my thesis and for copying to be done at the discretion of the archives' librarian and/or the College library.

_____ _____

Signature Date

TISSUE SPECIFIC EFFECTS OF *βFTZ-F1* LOSS-OF-FUNCTION ON THE EARLY GENE *E93* TRANSCRIPTION DURING DROSOPHILA MELANOGASTER METAMORPHOSIS

By

Anh Hoang

A paper Presented to the Faculty of
Mount Holyoke College in Partial
Fulfillment of the Requirements for
the Degree of Bachelors of Arts with
Honor

Program in Biochemistry
South Hadley, MA 01075

May, 2006

This independent work was carried out under the direction of Associate Professor Craig Woodard for 8 credits.

The research was funded by Mount Holyoke College Biology Department Grant

For *Ba, Má, Nguyên, and Họa*
Who teaches through examples,
Inspires me to push further,
And reminds me to laugh.

ACKNOWLEDGEMENTS

I would like to acknowledge the people who have made this study possible. First and foremost, special thanks to my "fearless leader," Professor Craig Woodard. His endless enthusiasm and support has inspired me to tackle real-time PCR and to continue with the project during troubled times.

Another special thanks to my partners in crime, Rachel Monyak and Chisanga Lwatula. They have spent many weekends and nights dissecting and analyzing results beside me. Also, thanks to my lab mates, Jodi McKenzie, Lisa Ng, Devi Yalamanchili, Hafsa Rahman, and Tina Fortier, for their friendships, supports, and laughters.

And finally, thanks to my cheerleading network: Clint Lindsay, Thang Dao, and Farah Siddique. They have endured my late night panic calls, listened to my complaints, and treated me with ice creams during stressful times.

TABLE OF CONTENTS

LIST OF FIGURES

LIST OF TABLES

ABSTRACT

Steroid hormones, in conjunction with their receptors, regulate the transcription of target genes in higher organisms. During *Drosophila melanogaster's* metamorphosis, two pulses of the steroid hormone 20-hydroxyecdysone (ecdysone) direct both morphogenesis and the destruction of tissues by programmed cell death. An increase in ecdysone titer at the end of the third larval instar triggers puparium formation, marking the onset of metamorphosis. As a result, the anterior larval muscles and larval midgut undergo apoptosis (Broadus, 1999).

Roughly ten hours after puparium formation (APF), another ecdysone pulse induces the prepupal-pupal transition during which the larval salivary glands undergo programmed cell death and leg imaginal discs complete their extension. Induced by these ecdysone pulses are the early genes, namely *Broad Complex (BR-C), E74A ,*and *E75A.* These genes encode transcription factor for genes involved in tissue morphogenesis and programmed cell death. In addition to these genes, the gene *E93* is expressed during the prepupal ecdysone pulse. The gene *E93* induces programmed cell death of the salivary land and midgut (Lee, 2002). During the interval of low ecdysone titer in mid-prepupae, the gene β*FTZ-F1* is expressed. This gene is believed to provide the early genes with the competence to respond to ecdysone (Woodard, 1994).

This experiment examines RNA isolated from salivary glands, midgut, hindgut and fat from animals aged at 10 and 12 hours APF. The expression level of *E93* in control (w^{1118}) animals was compared to *βFTZ-F1* loss of function mutants to determine if *βFTZ-F1* is required for the proper expression of *E93*. Real Time PCR was used to quantify the amount of *E93* mRNA in these tissues at specific metamorphic stages. The comparative C_T ($\Delta\Delta C_T$) analyses of relative real-time PCR results showed an underexpression of *E93* at 10 hrs APF in hindgut and salivary gland tissues of *βFTZ-F1* mutants, suggesting that *βFTZ-F1* was necessary for the expression of *E93.* Both midgut and fat body tissues of *βFTZ-F1* mutants showed similar expression as control animals. This indicates that *βFTZ-F1* was not necessary for the expression of *E93* in these tissues in late prepupae.

INTRODUCTION

Steroid hormones participate in various developmental processes by signaling cell proliferation, cell differentiation, and cell death. In higher eukaryotes, these activities work to control development and to maintain homeostasis. In humans, testosterone and estrogen participate in the development of sex-specific structures. For example, testosterone is responsible for the development of secondary male sex characteristics also called the androgenic functions of testosterone. In insect, steroid hormones also trigger cell proliferation, cell differentiation, and cell death (Riddiford, 1993). In *Drosophila* metamorphosis, the destruction of most larval tissues is necessary for the transition of a larva into an adult fly.

Steroid Hormones:

Hormones are chemicals produced in one organ that act on another region of the body through the transport in the circulatory system. With the exception of retinoic acid, steroid hormones are all derived from cholesterol and are lipid soluble (Mangelsdorf *et al.,* 1995). All steroid hormones contain the same cyclopentanophenanthrene ring and atomic numbering system as cholesterol (with the exception of vitamin D). Its lipophilic nature allows it to diffuse fairly freely from the blood through the cell membrane and into the cytoplasm of target cells (Yamamoto, 1985) (Figure 1).

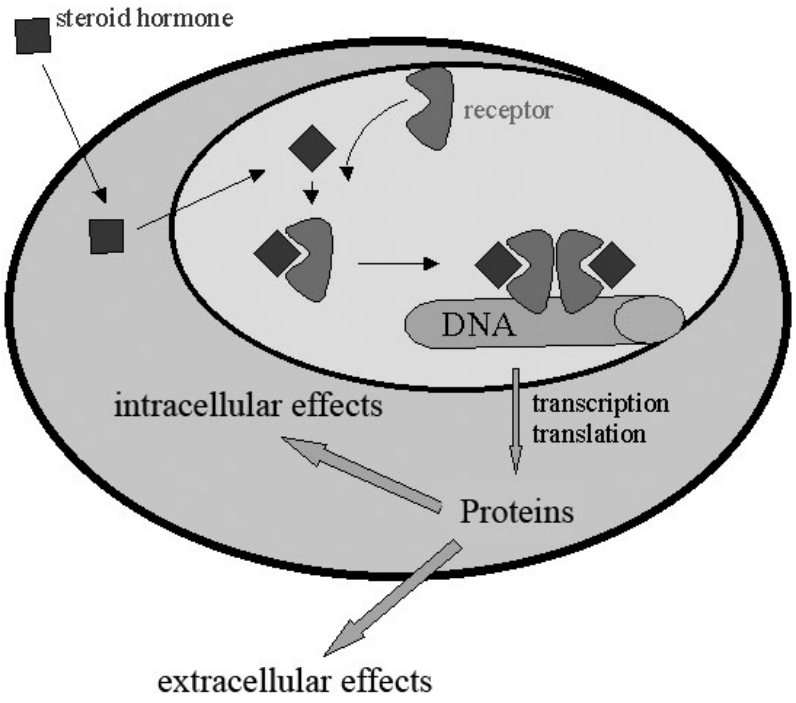

Figure 1. Mechanism of Action of Steroid Hormones. The steroid hormone penetrates the cell membrane and moves through the cytoplasm to the nucleus. It then couples with the receptor protein, forming a hormone receptor complex. The steroid receptor complex in turn enters the nucleus where it binds to specific chromosomal enhancers to induce or repress the transcription of their associated gene (VCU, 2000).

In the cytoplasm, the hormone binds to specific receptors, resulting in the dimerization of the receptors. Dimerization occurs when two subunits join to form a functional DNA-binding unit that enters the cell nucleus (Mangelsdorf *et al.,* 1995). The binding of hormone with its receptor induces an allosteric change which increases the affinity of the hormone-receptor complex for a specific site in chromatin, thereby activating the complex.

The activated Steroid Hormone Receptors (SHRs) binds to a palindromic DNA sequence, referred to as the Hormone Response Element (HRE). Steroid receptors share regions of close structural and/or functional homology which are called domains. For steroid receptors, these domains correspond to the amino-terminal region (A/B domain), DNA binding zinc finger region (C domain), hinge region (D domain) and C-terminal ligand-binding region (E/F domain) (Figure 2a). The amino terminal consists of a conserved DNA binding domain (DBD) comprised of 66 amino acids. This region contains segments of protein which form a three dimensional structure in which two cysteins and either two histidines or cysteins are orientated so as to bind a zinc atom (Figure 2b) These regions are referred to as zinc fingers. The resulting protein structure of the zinc fingers is shaped so that it can bind to the major groove on a DNA helix (Alberts, 2002). The binding of SHRs to HREs triggers the transcription of specific genes (Aranda and Pascaul, 2001).

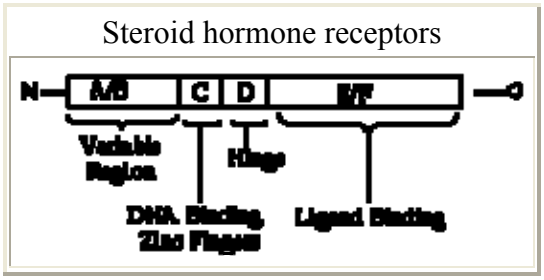

Figure 2a: Diagram of nuclear hormone receptor. The DNA binding domain (domain c), and the ligand binding and dimerization domain (domain E/F) are conserved. The other three domains (domain A/B and domain D) are variable. The amino-terminal region makes up domain A/B and the hinge region is domain D (Messer, 2000).

Figure 2b. Diagram of zinc fingers within DNA binding domain. Left. Zinc covalently binds to two cysteines, indicated by the solid balls; and two histidines or cysteines, indicated by the striped balls and solid balls, respectively, to form zinc fingers. Right. Protein zinc fingers binding DNA helix (Messer, 2000).

20- hydroxyecdysone:

In larvae of cyclorrhaphus diptera such as *Drosophila,* the prothoracic gland, the corpus allatum, and a third glandular tissue, the corpora cardiaca are joined to form the so-called ring gland. The ring gland is located dorsocephally between the two brain hemispheres. Its lateral extremities encircle the aorta like a ring, and thus, the structure has been given the name "ring gland."

In *Drosophila melanogaster*, the ring gland secretes two major ecdysteriod: α-ecdysone and 20-deoxymakisterone A (Ridiford, 1993). These hormones are largely inactive. 20- hydroxyecdysone (referred to here as ecdysone) is the product of the α-ecdysone conversion in the peripheral tissues and is the only known physiologically active steroid hormone in *Drosophila melanogaster* or *Drosophila*. Genetic studies suggest that ecdysone directs both morphogenesis and the destruction of tissues by programmed cell death in the fruit fly (Lee, 2002). Ecdysone directly induces a set of early regulatory genes that repress their own expression and induce a set of late secondary-response genes (Thummel, 2001*).* Induction of molting in the fruit fly coincides with the release of ecdysone in carefully timed spurts, corresponding with major morphological transitions.

Ecdysone consists of a three-membered ring attached to a single five membered ring characteristic of all steroid hormones (Figure 3) (Aranda and Pascual, 2001). Its lipid solubility allows it to diffuse through the plasma

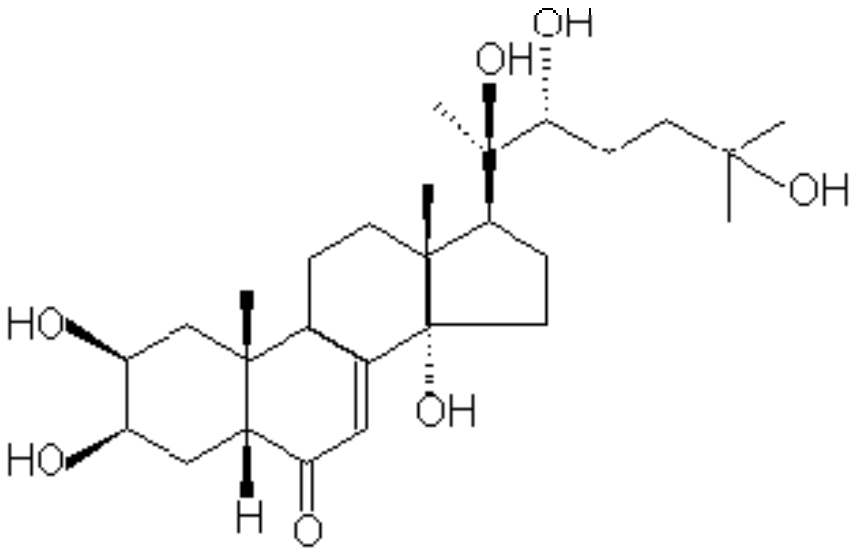

Figure 3. Chemical structure of 20-hydroxyecdysone (ecdysone). Ecdysone has the basic steroid characteristics: three six-membered rings attached to a single five-membered ring.

membrane of target cells where it binds to its receptor protein and induces an allosteric change in the receptor.

Ecdysone exerts its effect through the heterodimeric receptor complex encoded by the *Ecdysone Receptor (EcR)* and the *ultaspiracle (usp*) genes *(*Koelle *et al.,* 1991). USP has no known ligand, but it is the *Drosophila* homolog of the mammalian retinoid X receptors (Oro *et al*., 1990*).* Heterodimerization is required for these proteins to bind with ecdysone (Koelle *et al.,* 1992). Antibodies staining of salivary land polytene chromosomes showed a colocalization of EcR and Usp to many ecdysone-inducile puff loci (Talbot, 1993).

There are two types of consensus half-sites that are used by essentially all nuclear receptors: 5' –AGGTCA -3' and 5' –AGAACA -3' (Horner *et al.,* 1995). Binding selectivity depends on the geometry and spacing of the half-sites. The EcR and Usp complex mediates transcription through a pseudo-palindromic response element that resembles inverted repeats of 5'-AGGTCA-3' separated by one base pair. Both protein units belong to the superfamily of hormone receptors, ligand-dependent transcription factors that contain the DNA-binding domain (DBD) and the ligand-binding domain (LBD) (Devarakonda, 2003).

Thus far, nine *Drosophila* genes belonging to the nuclear hormone receptor superfamily have been identified*: EcR, usp, tll, svp, E75, E78, FTZ-F1, DHR3, and DHR39.* These genes have two C_2C_2 zinc fingers serving as a

sequence-specific DNA binding domain which includes the P box that helps determines the specificity of binding to target sequences. In addition, present in this family is a less conserved dimerization domain near the C-terminus. This region contains conserved heptad repeats of hydrophobic amino acids that play a role in mediating dimerization (Forman and Samuels, 1990). Genetic studies showed that *tll* participates in early embryonic pattern formation (Pignoni et al., 1990), while *svp* is involved in proper pattering of the adult eye (Mlodzik et al., 1990). Of the remaining seven genes, six function in the ecdysone regulatory hierarchies activated at metamorphosis: *: EcR, usp, βFTZ-F1, E75, E78,* and *DHR39.* These genes are mapped to salivary gland puff loci (Lavorgna *et al.,* 1993; Woodard *et al.,* 1994).

Ashburner's model:

In the early 1950s, Beermann observed that the localized increase in chromosome diameter, known as puffs, found in polytene chromosomes of *Diptera* occurred in a manner specific both to tissues and to developmental stages. A decade later, Becker showed that the activity of some puffs were under the control of hormones.

In 1967, Ashburner observed a pattern of puff formation in the giant larval salivary gland polytene chromosome. He described four classes of puffs: the intermolt puffs, the early puffs, early-late puffs, and late puffs. The intermolt puffs are active at the beginning of the response to ecdysone and thereafter regress. The early puffs are induced within minutes by ecdysone,

while the early-late puffs are induced with a delay of roughly two hours. The late puffs appear from three hours onward (Ashburner *et al.,* 1972).

Ashburner *et al. (*1974) observed that a small set of early larval puffs appear after exposure to ecdysone in the absence of protein synthesis. These puffs persisted for several hours in the presences of the hormone and later regressed. Puff 74E contains two genes, *E74A* and *E74B*. Puff 75B contains three genes, *E75A, E75B,* and *E75C* (Burtis *et al., 1990).* Puff 2B5 contains the gene *Broad-Complex (BR-C),* which encodes several members of the zinc-finger family (Dibello *et al.,* 1991).

The appearance of the early puffs is dependent on ecdysone exposure time. Induction of the early puffs is unaffected by the protein synthesis inhibitor cycloheximide. This suggested that the induction of the early puffs is a primary response to ecdysone exposure. Following the appearance of early puff by six hour was a set of late larval puffs. The timing and size of these late puffs is dependent on the expression of early puffs (Ashburner *et al.,* 1974). These late puffs remain transcribed throughout puparium formation. Based on these observations, Ashburner and his colleagues developed a model for the genetic regulation of polytene chromosome puffing by ecdysone in which the hormone, in conjunction with its receptor acts directly on DNA to stimulate the transcription of early genes while repressing the expression of the late genes (Figure 4). These early genes were hypothesized to encode

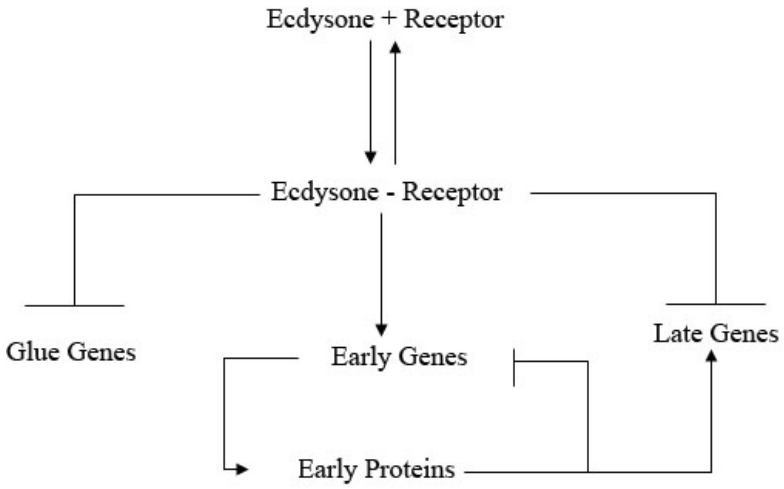

Figure 4. Transcriptional hierarchy induced by ecdysone. Ecdysone binds to its receptor to form the ecdysone-receptor complex. This complex activates early genes and represses a set of late genes and glue genes. The products of the glue genes act as an adhesive to immobilize the animal for puparium formation. The protein products of the early genes then activate the late genes. The products of the early genes repress their own expression (Ashburner, 1974).

regulatory proteins that repress their own activity and induce an over 100 additional late puffs. The late genes products play a more direct role in directing salivary gland programmed cell death.

Early Genes:

During *Drosophila's* third instar larval development, pulses of ecdysone activate three distinct sets of genes in the salivary glands, represented by puffs in the polytene chromosomes. One of the first sets induced genes are the intermolt genes. These genes encode a protein glue that the animal uses to adhere itself to a solid substrate for metamorphosis. These genes are repressed at puparium formation while a pulse of ecdysone induces a small set of early genes, including *Broad-Complex (BR-C), E74, E75.* These genes encode sets of related DNA-binding proteinsthat control the expression of downstream death genes (Segraves, 1988; Urness and Thummel, 1990; Huet *et al*., 1993; von Kalm *et al.,* 1994).

E74, a member of the *ets* protooncogene family, encodes two proteins, E74A and E74B. These proteins contain a common-terminal ETS DNA-binding domain (Burtis *et al.,* 1990). *E74* is an ecdysone primary-response gene contained within the 74EF early puff. In addition, *E74* regulates distinct sets of secondary-response genes in the larval and prepupal salivary glands (Fletcher and Thummel,1995).

Loss-of-function mutations of *E74A* or *E74B* are predominantly lethal during prepupal and pupal development, suggesting that these genes function

during metamorphosis (Fletcher *et al.,* 1995). Phenotypic analysis reveals that *E74* function is required for both pupariation and pupation, and for the metamorphosis of both larval and imaginal tissues (Fletcher *et al*., 1995). The *E74B* pupal lethal mutant phenotype includes cryptocephalic head structures and incomplete appendage elongation.

BR-C is an early ecdysone-inducible gene that encodes a family of DNA binding proteins (DiBello et al., 1991). *BR-C* is involved in imaginal disc evagination and fusion (Kiss et al., 1998), and proper development of thoracic muscle (Restifo, 1992). Mutation in *BR-C* result in reduced levels of ecdysone-induced *E74A, E75A,* and *BR-C* transcription in late third instar larvae (Karmin *et al.,* 1993).

BRC and *E74* are induced directly by ecdysone and both encode families of transcription factors that regulate ecdysone primary and secondary-response genes. Analysis of the morphological and molecular phenotypes of *BRC* and *E74* double mutants suggest that these genes work together, producing both novel and synergistic effects (Flethcer, 1995).

The ecdysone-inducible E75 gene responsible for the 75B puff encodes a family of proteins which are members of the steroid receptor superfamily. *E75* encodes three proteins that are isoforms of each other. All three isoforms have identical DNA binding domain and ligand binding domain in their c-terminal sequences (Segraves and Hogness, 1990). Various classes of E75 mutations lead to a variety of phenotypes including embryonic head involution defects, larval molting defects, and aberrant metamorphosis.

Drosophila melanogaster and Ecdysone action:

Drosophila melanogaster is roughly 3mm long. It has only one known active steroid hormone, ecdysone, making it an ideal model organism to study steroid hormone function. In addition to its well characterized genome, its life cycle takes 10-12 days at 25 degrees Celsius (Figure 5). This consists of an embryonic, three larval, a prepupal, and pupal stage. The fruit fly's genome contains three pairs of autosomes and one pair of sex chromosomes (Bodenstein, 1965).

The embryo develops one day after fertilization and hatches into a larva (Bodenstein, 1965). The larva eats, grows and undergoes three larval stages, referred to as first, second, and third larval instars. The first and second and second and third larval instar are separated by molting, which required the entire cuticle of the animal to shed and rebuilt. Each larval instar is characterized by an increase in size from the previous instar (Bodenstein, 1965). Two days into the third larval instar, a high ecdysone pulse triggers the transition of the larva into a non-feeding prepupa (Richards, 1991). At this stage, the animal anchors itself to a dry location, making it immobile. Animals at this stage are characterized by their white cuticles and everted spiracles. This stage lasts for roughly fifteen minutes and referred to as puparium formation, marking the end of the larval stage and the beginning of the prepupal stage and the beginning of metamorphosis. The onset of puparium

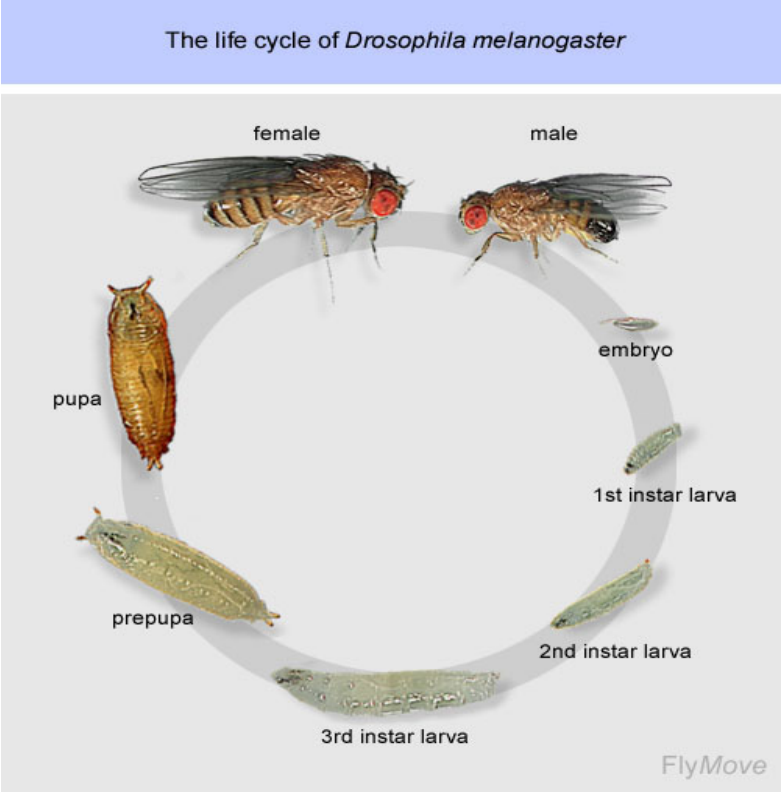

Figure 5. The life cycle of *Drosophila melanogaster*. The fruit fly's life cycle lasts for 10-12 days, and consists of the embryonic, three larval, a prepupal, and pupal stage. The first three stages are each one day long. The animal molts at the end of the second instar to form the third instar. The animal feeds for two days then is transformed into a motionless prepupa. Metamorphosis includes the prepual stage, which lasts 12 hours, followed by the three and a half day pupal stage. The end of metamorphosis occurs at the end of the pupal stage. The adult fly ecloses from the pupal case at this time.

.

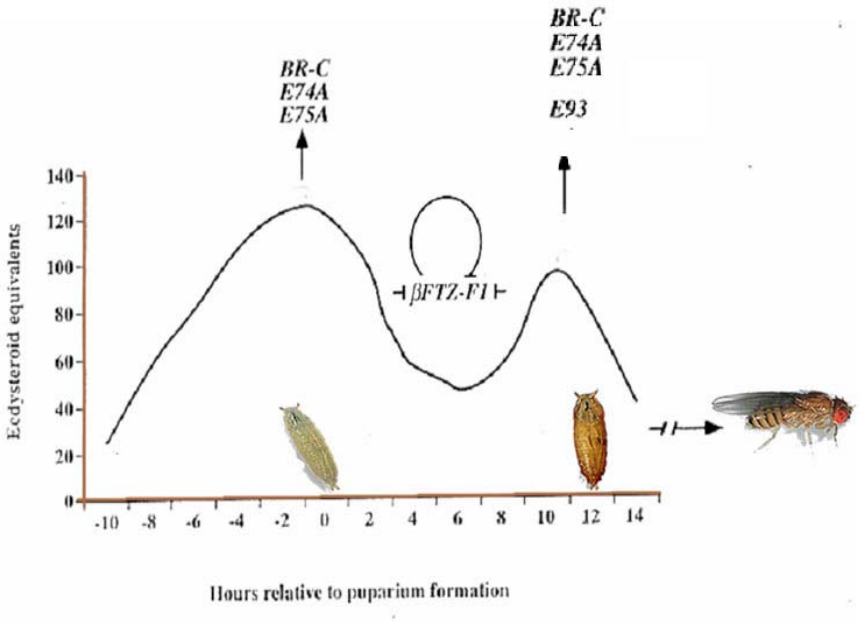

Figure 6. Ecdysone action during *Drosophila melanogaster* development. A pulse of ecdysone at the end of the larval development triggers puparium formation, initiating the prepupal stage of development. This pulse of ecdysone triggers the expression of early genes, *Broad Complex (or BR-C), E74A, and E75A.* Ten hours after puparium formation, another pulse of ecdysone induces the prepupal-pupal transition. This pulse of ecdysone induces a set of early genes, *BR-C, E74, E75A ,* and *Eip93F (E93),* in the salivary glands. An orphan member of the nuclear receptor superfamily, *βFTZ-F1,* is expressed during the period of low ecdysone concentration in midprepupae. *βFTZ-F1* functions as a competence factor that allows the prepupal pulse of ecdysone to reinduce the early genes and initiates transcription of the gene *E93(*Broadus *et al.,* 1999, Woodard *et al.*, *1994).*

formation is referred to as zero hours after puparium formation (APF). During this stage, the larva becomes shorter and broader, while anterior spiracles evert for gas exchange purposes.

An increase in ecdysone titer at the end of the third larval instar triggers puparium formation. This marks the onset of metamorphosis. As a response, the anterior larval muscles and larval midgut undergo apoptosis (Broadus *et al,* 1999). This pulse of ecdysone triggers the expressions of early genes, *Broad Complex (BR-C), E74A, and E75A,* in the salivary glands. Shortly after puparium formation, this ecdysone titer decreases (Figure 6).

Roughly ten hours after puparium formation, another ecdysone pulse induces the prepupal-pupal transition during which the salivary glands undergo programmed cell death and leg imaginal discs complete their extension. In addition, this ecdysone titer also induces adult head eversion (Jiang *et al.,* 1997)

Induced by the prepupal pulse of ecdysone are the expression of early genes, *BR-C, E74,* and *E75*. A few early genes are induced by ecdysone in a stage-specific manner in prepupae. One of these is the stage specific gene *E93. E93* encodes a transcription factor and is induced directly by ecdysone in the late prepupal salivary glands but was not present during the first ecdysone titer.

The expression of *E93* follows a period of low ecdysone concentration. It is thought that one or many proteins that are repressed by ecdysone and expressed in the mid-prepupae provide competence for the

early genes to response to ecdysone (Richards, 1976). The mid-prepupal puff, puff 75CD, appears as the ecdysone level drops three to eight hours APF. In Richards' (1976) study of cultured salivary glands,he observed that glands isolated from prepupae aged zero, two, and four hours did not respond, by puffing at 74EF, 75B, and 93F, to ecdysone. However, glands dissected from six hours prepupae were competent. Ecdysone cultured glands show maximal response within two hours of culture.

Puffs of ten hours prepupa are induced by ecdysone, but only if the glands have previously been at least three hours in the absence of ecdysone. Also, regression of the 75CD puff was observed with the addition of ecdysone to mid-prepupal salivary glands (Richards, 1976). Richard concluded that competence is acquired in the absence of ecdysone, during the mid prepupal period, but not during period of high ecdysone concentrations (2.4×10^{-6} M).

An orphan member of the nuclear receptor superfamily, *βFTZ-F1* is thought to be the mid-prepupal competence factor. Before the prepupal ecdysone titer, *βFTZ-F1* is transcribed (Lavorgna *et al.,* 1993). Woodard and colleagues (1994) detected *βFTZ-F1* transcript within four hours and continued to be present through eight hours in cultured zero hour prepupae in the absence of ecdysone. This pattern of *βFTZ-F1* expression mirrors that of the 75CD puff, which, under the same condition, appears at roughly three hours and remains present for at least six hours (Richards, 1976). In *vivo,* partial competence was observed by five hours APF, and full competence

was achieved in seven hours prepupae. This pattern parallels the temporal pattern of *βFTZ-F1* transcription in salivary glands (Woodard *et al.,* 1994).

Ectopic expression of *βFTZ-F1* in late-third instar larvae increased the level of ecdysone-induced *BR-C, E74A, E75A* and *E93* transcriptions and premature induction of the stage-specific 93F early puff and *E93* transcription (Woodard *et al*., 1994). From this and similar observations, Woodard and colleague proposed the following model for acquisition of competence. The 75CD puff activation requires the induction of one or more proteins in the late-third instar larvae (Richards, 1976). Upon its induction in mid-prepupae, *βFTZ-F1* binds to its cognate sites in the genome, including *BR-C, E74, E75* (Lavorgna *et al.,* 1993) and *E93*. This provides these genes with the competence to be induced by ecdysone in late prepupae (Woodard *et al.,* 1994).

Eip93F (E93)* Regulates Programmed Cell Death*:

The role of *βFTZ-F1* in steroid-activated larval cell death appears to be indirect, functioning as a competence factor for prepual responses to ecdysone (Woodard *et al.,* 1994). Instead, one or more stage-specfic regulators that is induced by ecdysone at the end of the prepupal development directly determines the stage specificity of salivary gland cell death. The early gene *E93* is an ideal candidate for this function. It is induced as a primary response to ecdysone in a stage- and tissue-specific manner

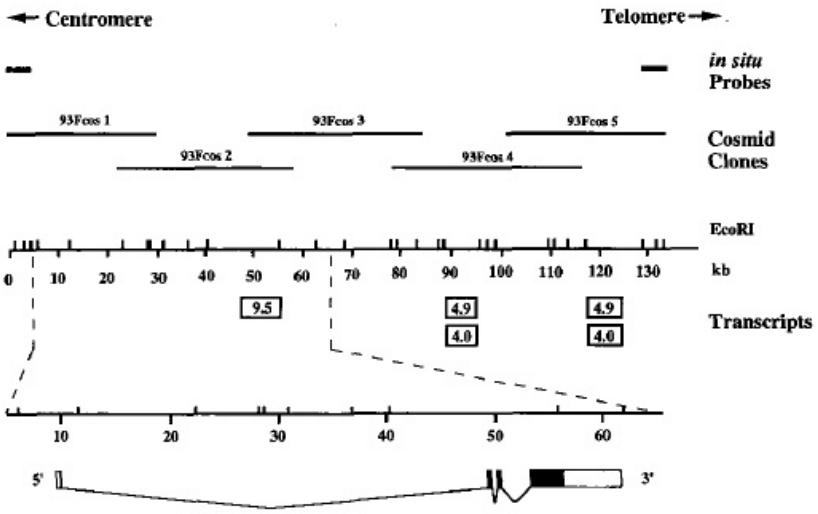

Figure 7. Diagram of the gene *E93*. *E93* spans roughly 55 kb of genomic DNA and encodes a 146 kDa protein. This protein possesses several characteristics of known *Drosophila* transcription factors. It is thought that *E93* is necessary for the destruction of larval midgut and salivary glands in response to ecdysone (Lee *et al.,* 2000).

(Baehrecke and Thummel, 1995). *E93* is located at position 93F (Richards, 1976). Baehrecke and Thummel (1995) were able to isolate and characterized as the gene *E93* from this puff (Figure 7). *E93* is directly induced by ecdysone in prepupal salivary glands and contains a transcription unit of 55kb of genomic DNA which encodes for a novel protein of 146 kDa (Baehrecke & Thummel, 1995). This protein is expressed in doomed larval cells.

The precise temporal and spatial regulation of *E93* sets it apart from other early genes. *E93* responds to ecdysone in a tissue and time-specific manner. Its mRNA was detected in fat body and midgut tissues in newly formed prepupae (Lee *et al.,* 2000). Expression of *E93* continues in these tissues following the prepupal ecdysone pulse, with an increase expression in the fat body. *E93* is also expressed in CNS and imaginal discs of late prepupae (Baehreck & Thummel, 1995). In studies using cultured prepupal organs, Baehrecke and Thummel (1995) were able to show that ecdysone is responsible for an increase in *E93* expression in salivary glands, fat body, and gut, while *E93* transcription in the CNS occurs independently of ecdysone. Also, Lee and colleagues (2000) observed that *E93* mutant salivary glands fail to die and that expression of *E93* is sufficient to restore this cell death response. These observations suggested that *E93* may function as a stage-specific transcription factor that initiates histolysis in the salivary gland (Baehrecke and Thummel, 1995).

β*FTZ-F1* Provides Competence to Early Genes to Respond to Pulses of Ecdysone:

In the presence of β*FTZ-F1,* the late prepupal ecdysone pulse induces the expression of early genes, *BR-C, E74A, E75A* and *E93,* prior to larval salivary gland programmed cell death (Broadus *et al*., *1999;* Woodard *et al.,* 1994) and is believed to be a mid-prepupal competence factor for both genetic and biological responses to the prepupal ecdysone pulse, including salivary gland cell death (Woodard *et al.,* 1994, Broadus *et al.,* 1999).

Despite its large role in development, little is understood about the mechanism behind the acquisition of competence. Molecular mechanisms have been defined in two areas, both based at the transcriptional level: one, competence is achieved through the expression of specific receptors, or cofactors that regulate activity (Shi *et al.,* 1996; Puigserver *et al.,* 1998); and two, competence can be regulated through the expression of histone H1 subtypes or phosphorylation of histone H1(Steinbach *et al.,* 1997; Lee and Archer, 1998).The absence of the receptor or its cofactor will inhibit a cell's response to a signal, while histone modification enables transcription through alteration of chromatin structures.

Four genetic studies have confirmed that β*FTZ-F1* functions as a competence factor of ecdysone during prepupal development. One, β*FTZ-F1* is expressed during the interval of low ecdysone titer in mid-prepupae. Two, β*FTZ-F1* proteins bind to many ecdysone-regulated puffs in the salivary gland polytene chromosomes of late prepupae (Lavorgna *et al.,* 1993). Third,

ectopic expression of β*FTZ-F1* increases the ecdysone-induction of early genes and directs premature *E93* expression (Woodard *et al.,* 1994). Fourth, β*FTZ-F1* loss-of-function mutants display defects in the events of the prepupal-pupal transition. This includes adult head eversion, leg elongation, and salivary gland cell death (Broadus *et al.,* 1999).

FTZ-F1 encodes two protein isoforms that have distinct temporal patterns of expression: α*FTZ-F1* and β*FTZ-F1* (Lavorgna *et al.,* 1993). The FTZ-F1 protein is a member of the steroid receptor superfamily. α*FTZ-F1* is supplied maternally. It functions as a cofactor for *FTZ* during segmentation (Guichet *et al., 1997).* β*FTZ-F1* expression is observed in late embryos prior to each larval molt and mid-prepupae (Yamada *et al.,* 2000). The prepupal transcription of β*FTZ-F1* parallels the puffing pattern at 75CD. This suggests that β*FTZ-F1* contributes to 75CD puff formation (Lavorgna *et al.,* 1993).

The β*FTZ-F1* protein is encoded by an open reading frame of 816 codons and has a molecular mass of 88 kD (Lavorgna *et al.,* 1993). It is identical to the α*FTZ-F1* in the carboxyl-terminal, two-thirds of the protein. The amino-terminal region differs between two isoforms. This region is enriched with glutamine, asparagines, and serine residues in β*FTZ-F1*, but rich in serine, alanine, and threonin residues in the α*FTZ-F1* (Lavorgna *et al.,* 1993).

Midgut and salivary glands cell death:

Cell death is necessary for normal development and maintaining homeostasis (Jacobson *et al.,* 1997). Disruption in programmed cell death

regulation may result in lethal consequences. Necrosis is cell death due to external injury. Unlike necrosis, programmed cell death is activated inside the cell through a genetically conserved regulatory pathway, which does not elicit inflammatory responses (Lockshin and Zakeri, 1991). Steroid hormones appear to regulate programmed cell death in *Drosophila* through mainly apoptosis and autophagy (Thummel, 2001).

Ecdysone exerts its effect on *Drosophila* development by triggering stage and tissue specific regulatory hierarchies. The stage specificity of cell death responses is illustrated by the salivary glands and larval midgut. The midgut initiates cell death in early prepupae while in the larval salivary glands, cell death occurs in early pupae, following the prepual pulse of ecdysone (Jiang *et al.,* 1997) (Figure 8). During the prepupal-to-pupal transition, the larval foregut epithelium is replaced by the adult foregut and larval salivary glands are destroyed by programmed cell death (Bodenstein, 1965).

The midgut and salivary glands exhibit markers of programmed cell death following the prepupal pulse of ecdysone. This includes staining by acridine orange and DNA fragmentation (Jiang *et al.,* 1997). Lee and Baehrecke showed that the expression of the baculovirus caspase inhibitor p35 results in the failure of midgut and salivary glands to degenerate. Roughly 89% of these glands progress normally to a late stage in autophagy but do not proceed past DNA fragmentation. The remaining 11% of salivary glands are blocked at an early stage of autophagy with large autophagic vacuoles having

intact plasma membranes. When the p35 expression level was increased, this ratio did not change. This suggests that caspases are required for autophagic destruction of salivary glands. In addition, transcription of cell death inducers (*rpr* and *hid)* increases preceding both larval midgut and salivary gland death (Lee *et al.,* 2002). The expression of *rpr* appears to be restricted to dying cells. The ectopic expression of this gene is sufficient to induce caspase-dependent programmed cell death (Grether *et al.,* 1995).

Drosophila metamorphosis requires the reorganization of midgut structure. This process includes the destruction of larval cells and the proliferation and morphogenesis of adult midgut tissues (Robertson, 1936). This dramatic change may be a result of the changes in diet between the larval and adult stages. For example, the larva feeds on decaying fruit while the adult consumes a semi-liquid diet. Lee and colleagues (2002) observed characteristic of autophagy in the third larval instar midgut following an increase in ecdysone levels. The adult midgut epithelium is already formed by the time larval midgut cell death reaches advanced morphological stages. The digestive system is essential for the survival of the animal, thus, it may be critical to develop the adult midgut epithelium before the destruction of the larval midgut. The *Drosophila* midgut dies by autophagic programmed cell death. Advanced signs of autophagy are not observed until larval midgut has been isolated from the haemocoel by the developing adult midgut epithelium (Lee *et al.,* 2002). Larval midgut death differs from larval salivary gland death. Ecdysone elicits midgut to die at the same stage as when salivary

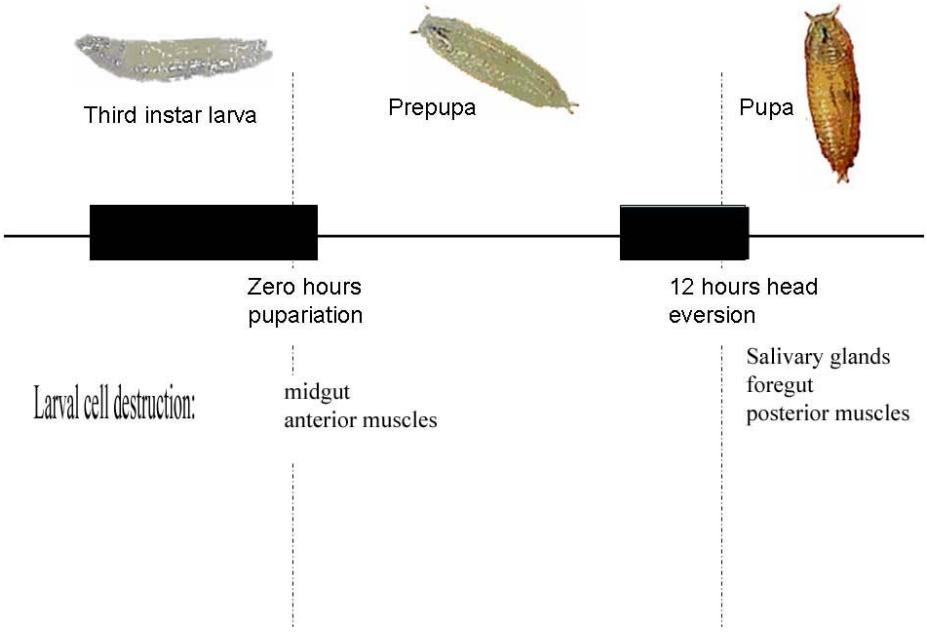

Figure 8. Timeline of larval cell destruction. Fluctuations in ecdysone titer, indicated by the shaded bars, trigger larval cell destruction during *Drosophila* metamorphosis. The first ecdysone titer triggers cell death in midgut and anterior muscle tissues. The second ecdysone titer triggers cell death in salivary glands, foregut, hindgut and posterior muscles (Baehrecke, 2000).

glands synthesize and secrete polypeptide glue. Furthermore, future adult midgut cells are dispersed in the larval midgut epithelium, while adult salivary glands are restricted in one ring of cells (Robertson, 1936).It is thought that adult midgut cells utilize larval midgut as a substrate to develop around, while larval salivary gland is not necessary for adult salivary gland formation. Several differences exist between ecdysone-regulated midgut and salivary gland programmed cell death. First, these tissues are triggered to die by independent pulses of ecdysone (Jiang *et al.,* 1997). And second, dying larval midgut cells associate with future adult midgut cells within the epithelium of larval midgut (Robertson, 1936) while salivary gland cells do not associate with adult cells.

E93 and *BR-C* appear to be critical in the regulation of midgut cell death (Lee *et al.,* 2002). However, mutations in these genes produced different effects in salivary glands and midgut. *BR-C* appears to play a more important role in midgut death. Mutation in *BR-C* affects transcription of death inducer genes (*rpr, hid,* and *crq)*, but *E93* mutants only affect *dronc* transcription in midguts (Lee *et al.,* 2002). In addition, salivary gland death contains distinct features of autophagy (Jochova *et al.,* 1997). This includes an increase in acid phosphatase activity and an increase number and size of autophagic lysosomal vaculoles (Von Gaudecker *et al.,* 1974). This observation was confirmed by Lee and Baehrecke (Lee and Baehrecke, 2001).

Purpose

A primary goal of this study is to determine how a single hormonal signal of ecdysone can direct the distinct stage- and tissue-specific biological responses in *Drosophila melanogaster.* Exact timing and regulation of genes is vital during *Drosophila* metamorphosis. Thus, the ecdysone-induced responses of the early genes are essential to the survival of the animal. The current model of ecdysone action provides insight on metamorphosis requirements for the animal as a whole. However, little is known regarding tissue specific responses to ecdysone.

Up to date, the ecdysone action in the salivary glands and in whole animal has been studied. The current model of ecdysone action in the salivary gland shows that the expression of *βFTZ-F1* during the mid-prepupal, provides early genes with the competence to respond to the hormone. Ecdysone actions in other tissues are unclear. To further this research, this study will investigate tissue specific responses to ecdysone by examining the expression of the stage-specific gene, *E93*, in various tissues of *βFTZ-F1* loss-of-function mutants during *Drosophila melanogaster* metamorphosis.

In this experiment, *E93* mRNA transcript was measured from tissues isolated from salivary gland, midgut, hindgut and fat of mutants. These animals were aged to 10 and 12 hours APF, after the expression of *βFTZ-F1*. Quantitative Real-Time Polymerase Chain Reaction was used to quantify the amount of *E93* mRNA in these tissues. This technique is based on detection of a fluorescent signal that is proportional to the PCR products produced during

the amplification of a reaction. The comparative C_T ($\Delta\Delta C_T$) analyses method was used to analyze experimental data.

MATERIALS AND METHODS

Fly Stocks and Crosses:

βFTZ-F1 loss-of-function mutants contained deletions within the *βFTZ-F1* gene. These mutations include *FTZ-F1*^{17}, a hypomorphic mutation that specifically affects *βFTZ-F1* function. *FTZ-F1*^{17} homozygous prepupae express a reduced level of full length *βFTZ-F1* transcript compared to control prepupe(*w*^{1118}). This effect is a result of the deletion which extends upstream from a viable P element insertion site, P{(W^+,ry^+)H} 2-2 (Levis *et al.,* 1985), removing the *βFTZ-F1* regulatory sequence (Broadus *et al*., 1999). This deletion does not extend into the α*FTZ-F1* specific sequences because the abundance and size of α *FTZ-F1* transcript in the ovaries of *FTZ-F1*^{17} homozygous females are indistinguishable from wild type. Some *FTZ-F1*^{17} animals are able to survive until puparium formation, which allows a study of *βFTZ-F1* function during metamorphosis. *Df(3L)Cat*^{DH104} mutants has the *βFTZ-F1* gene deleted. *Df(3L)Cat*^{DH104} and *FTZ-F1*^{17} mutants were maintained over a balancer chromosome. The *Df(3L)Cat*^{DH104} */ TM6B, Hu e tb* animals have one functioning copy of the *βFTZ-F1* gene.

FTZ-F1^{17}*/ TM6B, Hu e tb* and *Df(3L)Cat*^{DH104} */ TM6B, Hu e tb* were crossed to obtain the genotype *FTZ-F1*^{17}*/ Df(3L)Cat*^{DH104}. These animals

show more severe phenotypes than *FTZ-F1*^{17} homozygotes and have one poorly functioning copy of the gene *βFTZ-F1*. Note that the hemizygous mutant pupae could be readily identified by the absence of the *Tubby* marker, which is carried on the balancer third chromosome. Animals possessing this marker will have a round short body.

Animal Staging and Phenotypic Analysis:

All flies were maintained on cornmeal agar food at 25° C. *FTZ-F1*^{17}*/ Df(3L)Cat*^{DH104}animals were collected at puparium formation (zero hour) and aged for 10 and 12 hours. Both mutant and control animals were allowed to develop on moist filter paper. These animals were dissected for salivary glands, gut, fat, CNS and imaginal discs in 1X Rob buffer solution (refer to appendix). Tissues were then homogenized in a mixture of 30 µl 1X Robb buffer and 300 µl TRIzol reagent from Sigma-Aldrich and stored at -80° C.

RNA isolation:

One microliter of linear polyacrylamide (GenElute LPA from Sigma-Aldrich) was added to each sample of previously homogenized tissue. The mixture of tissue and LPA was vortexed and transferred to a Phase Lock Gel-Heavy 2ml tube. 60 µl of chloroform was added and shook vigorously. The mixture was centrifuge at 4° C at 15,000 rpm for 10 minutes. The aqueous phase was transferred to a RNase-free tube. 160 µl of isopropanol was added and allowed to precipitate overnight at -20° C. The precipitated sample was centrifuged at 4° C at 15,000rpm for 20 minutes the following day. The

supernatant was removed. The pellet was washed with 500 µl ethanol(75%) and centrifuged at 4° C at 15,000 rpm for 5 minutes. The supernatant was removed. The pellet was dissolved in 5 microliters in 55° C and stored at -80° C. The qualities of the RNA were checked using the Agilent - 2100 Bioanalyzer.

Complementary DNA (cDNA) synthesis:

cDNA libraries represent the information encoded in the messenger RNA (mRNA) of a particular tissue or organism. RNA molecules are exceptionally labile and difficult to amplify in this form, thus, the conversion of RNA into stable DNA duplex (cDNA) is performed to conduct genetic studies.

Isolated mRNA from control and experimental animals were used to synthesize cDNA. A no-Reverse Transcriptase (RT) control and positive control using a different RNA from Invitrogen™ were performed to verify the effectiveness of the cDNA synthesis process. The reagents on table 1a were combined and placed in a water bath at 65° C for five minutes. Nine microliters of the reaction cocktail (Table 1b) was added to the previous mixture. The combined mixture was incubated for two minutes at 42° C. Following this incubation, one microliter of Superscript II RT (50 units/µl) was added to each sample. First-strand cDNA synthesis starts when the enzyme Superscript II RT, in the presence of nucleotides and buffer, finds a mRNA template and a primer. This enzyme converts the mRNA sequence into single stranded DNA equivalent.

Table 1a. cDNA reagents, part I. Reagents combined for each reaction and incubated at 65° C for five minutes.

components	volume added(µl)	Concentrations
RNA	1	1µg/µl
dNTP mix	1	10mM each dATP, dCTP, dGTP, dTTP)
Oligo dT	1	0.5 µg/µl
Rnase free water	7	
total	10	

Table 1b. cDNA reagent, part II. Components combined to previous mixture (table 1a) and incubated at 42° C for two minutes per reaction.

components	volume added(µl)	Concentrations
10X RT Buffer	2	200 mM Tris-HCL (pH 8.4), 500 nM KCL
$MgCl_2$	3	25mM
dTT	2	0.1 M
Rnase Out	1	40 units/µl

Following the addition of Superscript II RT, the mixture continued incubating at 42° C for 50 minutes. This was followed by incubation at 70° C for 15 minutes. The samples were then chilled on ice and centrifuged. One micoliter of RNase-H (2 units/ µl) was added to each reaction. PCR's sensitivity for cDNA can be increased by removing the RNA template from the cDNA:RNA hydrib molecules by digestion with RNase-H after first strand synthesis. RNase H will degrade the template mRNA which will result in a decreased in full-length cDNA synthesis and decreased yields of first-strand cDNA. The mixture was then incubated at 37° C for 20 minutes. CDNA was stored -80° C.

Polymerase Chain Reaction (PCR):

Primers and real time PCR probes for *E93* and *β-actin* were designed by Rachel Monyak and Chisanga Lwatula using the program Primer 3 and produced by Integrated DNA Technologies, Inc (IDT).

E93:

Left Primer: 5'- ACATTCATCAGCACGAGAGT -3'

Right Primer: 5'- GAGTCCATCGATGTCATTTT -3'

Probe: 5'-TCCCTTGAACTCTACA AGCTGCTGACCCA-3'

β-actin:

Left Primer: 5'-TCTAGGGTTATGCCCTT-3'

Right Primer: 5'-GCACAGCTTCTCCTTGATGT-3'

Probe: 5'-TGGTCGCGATTTGACCGACTACCTGATGAA-3'

These primer sets were optimized by performing PCR reactions on an annealing temperature gradient of 47-58° C. The primer set was further optimized by performing PCR reactions using various primer concentrations at the previously determined optimal temperature. PCR products were expected to be 200 base pairs for *E93* PCR product. PCR reactions were completed in 35 cycles of the following stages:

Denaturation: 95°C for 30 seconds

Annealing: 30 seconds

Elongation: 72°C for 30 seconds.

Real-time PCR:

A PCR reaction is broken down to three basic phases: exponential, linear, and plateau. During the exponential phase, the product is doubled at every cycle (assuming there is a 100% reaction efficiency). New and available reagents encourage exponential growth. As the reaction progresses, the reagents are consumed. As a result, the reactions slow down and the PCR products are no longer being doubled at each cycle, instead, the reaction enters a linear amplification phase. Eventually, the reactions slow down and plateaus. The rate at which each sample enters the plateau phase varies on the reaction kinetics for each sample. If three separate PCR reactions were performed using the same initial conditions, each sample's difference in reaction kinetic

may result in various time-point at which each reaction reaches the plateau phase. Then, measurements taken at the plateau phase may not truly represent the initial amount of starting target material. Thus, using the endpoint data to quantify level of expression will vary slightly between trials. Traditional PCR takes its measurement during the plateau phase while Real-time PCR takes its measured during the exponential phase of the PCR reaction.

Real-time PCR studies allow for the detection of PCR amplification during the early phases of the reaction. Traditional methods use agarose gels for the detection of PCR amplification at the final phase or endpoint of the PCR reaction. Endpoint PCR has limitations. This method is time consuming and results are based on size discrimination. In addition, endpoint PCR has poor precision, low sensitivity, low resolution, and requires post PCR process.

Quantitative real-time PCR can detect sequence-specific PCR products as they accumulate in "real time" during the PCR amplification process. As the PCR product increases, real-time PCR detects the products and quantifies the number of substrates present in the initial PCR mixture. This allows the comparison of expression level between different samples. That data output is expressed as a fold-change or a fold difference of expression level.

The method behind real time-PCR is based on the 5'-3' exonuclease activity of the *Taq* DNA polymerase, which results in cleavage of fluorescent dye-labeled probes. In our experiment, we used the TagMan® probes. The TagMan® probe is located between the two PCR primers. The probe sits in

the path of the *Taq* DNA polymerase as it starts to copy DNA. Degradation of the TagMan® probe by the *Taq* DNA polymerase cleaves the probe.

The TagMan® Probe is designed with a high-energy dye, the reporter dye, at the 5' end, and a low-energy dye, the quencher, at the 3' end. In this study the reporter dye 6-carboxyfluorescein (FAM) and the quencher dye Black Hole Quencher were used. When the probe is intact and excited by a light source, the reporter dye's emission is suppressed by the quencher dye due to the spatial proximity of the dyes. Cleavage of the probe by the 5' nuclease activity of *Taq* DNA polymerase increases the distance between these dyes, and thus the reporter dye fluoresces. The increase in reporter signal is captured by the Sequence Detection instrument and interpreted by the ABI software. The level of reporter signal is proportional to the amount of product being produced by a given sample.

β-actin, an endogenous control was used to normalize target quantities. An endogenous control is a gene sequence present in both experimental and control samples. *β-actin* serves as the internal control gene and used to normalize the PCRs for the amount of mRNA input. mRNA of equal amount for experimental and control samples were used in each reaction. Each real-time PCR reaction includes reagents listed in Table 2. Real-time PCR conditions are as follow: the reaction mixtures are heated to 50°C for 2 minutes and then heated to 95°C for 10 minutes. Following these heating steps, the reaction mixtures go through 40 cycles of 95°C for 15 seconds and 60°C for 1 minute.

Table 2. Reagents for real-time PCR reactions. The following reagents were combined for real-time PCR reaction. Total reaction volume was 50 µL. TagMan® Universal PCR Mastermix and probes (β-actin and *E93)* were purchased from Applied Biosystems (ABI).

Reagents	volume (µL)	initial concentration	final concentration
Taqman® Universal PCR Mastermix	25 (2X)		1X
Left Primer	1	.01 nM/ µL	200 nM
Right Primer	1	.01 nM/ µL	200 nM
Probe	1	. 01 nM/ µL	200 nM
cDNA template	1	500 µg/ µL	
nuclease free water	21		
Total:	50		

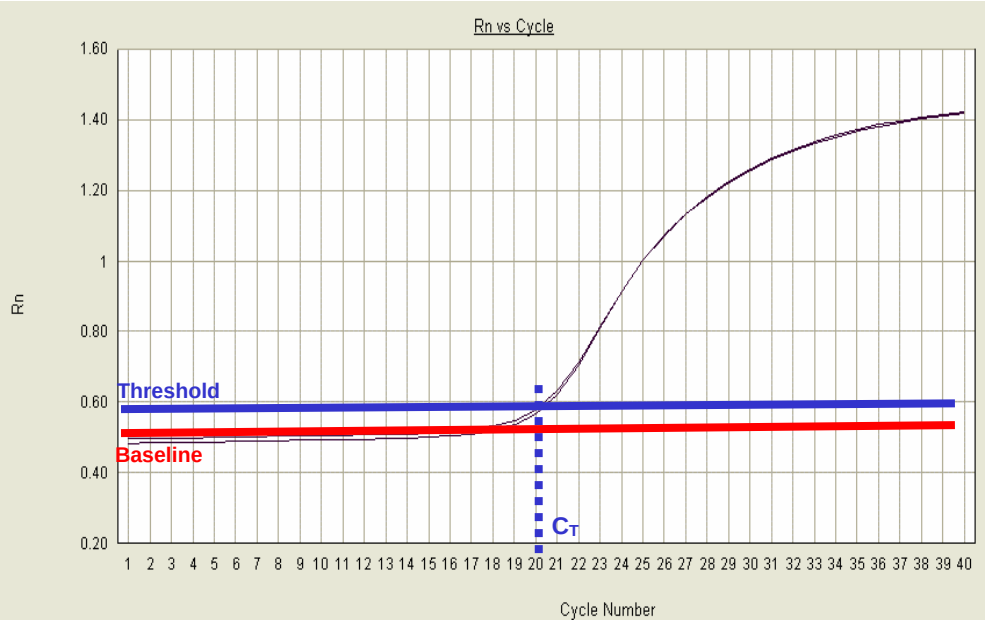

Figure 9. Example of real-time PCR amplification plot. The baseline level is the background fluorescence signal emitted during the early cycles of the PCR reaction before the detection of the PCR products. The threshold line is a level of normalized reporter signals that is used to determine the cycle threshold, C_T, in the real-time assays. The C_T is the cycle number at which the fluorescence generated within the reaction crosses the threshold line. C_T values are logarithmic and are used for quantitative analyses.

.

Figure 9 shows an example of a real-time PCR amplification plot. The threshold line is the level of detection at which a reaction reaches a fluorescent intensity above background fluorescence (baseline). The threshold line is set in the exponential phase of the amplification. The cycle at which the plot crosses the threshold is called the cycle threshold, C_T. The smaller the C_T value for a given gene, the higher the expression level of that gene. For example, if the amplification plot for the expression of gene A in salivary glands tissues shows a C_T value of 23, while the amplification plot of gene B in salivary glands tissues show a C_T value of 24, then this indicates that the expression of gene A is higher than the expression of gene B in the salivary glands at that time point.

Real-time PCR data analysis:

Two different methods of analyzing data from real-time PCR experiments exist: absolute quantification and relative quantification. Absolute quantification determines the input copy number of the transcript of interest. This is usually done by relating the PCR signal to a standard curve. This method of analysis is done when it is necessary to determine the absolute transcript copy number. Relative quantification determines the change in expression of the target gene relative to some reference group (i.e an untreated control).

The comparative C_T method ($\Delta\Delta C_T$) uses an arithmetic formula to perform relative quantification calculation and analysis. The relative change in gene expression determined from a real-time PCR experiment (normalized to an endogenous reference and relative to a calibrator) is calculated by the following equation:

$$2^{-\Delta\Delta CT}$$

Where in a 100% efficient reaction, the PCR product doubles after every cycle and $\Delta\Delta C_T = \Delta C_{T\ \text{test sample}} - \Delta C_{T\ \text{calibrator sample}}$. For the $2^{-\Delta\Delta CT}$ calculation to be valid, the PCR amplification efficiencies of the target and reference must be roughly equal. PCR amplification efficiency is the rate at which a PCR amplicon is generated, commonly expressed as a percentage value. For example, a 100% efficiency would indicate that a particular PCR amplicon doubles in quantity during the geometric phase of its PCR amplification.

The use of the comparative C_T method can be validated by observing how ΔC_T varies with template dilution. C_T values are obtained for each dilution for both experimental and reference samples. These values must be approximately equal. ΔC_T is determined by subtracting the C_T value of the reference sample from the experimental value ($C_{T\ \text{experimental}} - C_{T\ \text{endogenous}}$). The ΔC_T values are plotted vs. log input amount to create a semi-log regression line. The slope of this plot can be used to validate the experiment. In a

validated experiment, the slope of a ΔC_T vs. log input is < 0.1. If the slope is close to zero, the efficiencies of the experimental and reference genes are similar, and the $\Delta\Delta C_T$ method may be used to analyze the data.

PCR amplification efficiency is determined by producing a standard curve using *E93* and *B-actin* primer sets. PCR reactions were performed on various dilutions of whole animal mRNA input. C_T values of each reaction was determined and plotted against log of input. The slope of a standard curve is used to estimate the PCR amplification efficiency of a real-time PCR reaction. A slope close to -3.32 indicates 100% efficiency of the PCR reaction. This suggests a 100% efficient reaction will yield a 10-fold increase in PCR product every 3.32 cycles during the exponential phase of amplification ($\log_2 10 = 3.32$). Slopes more negative than this value indicate reactions that are less than 100% efficient. A slope more positive than -3.32 indicates sample quality or possible pipetting error. T-tests were performed to assess whether results from the comparative C_T method were statistically significant.

RESULTS

Primer optimization results:

Primers for the gene *E93* were optimized for PCR conditions by performing PCR reactions on an annealing temperature gradient of 47 – 58 °C. PCR products were subjected to electrophoresis (Figure 10a). As expected, *E93* PCR products were 200 base pair (bp) in size. Bright bands were observed at temperatures 48-50 °C and 58-60°C, which included IDT's suggested optimal temperature of 60 °C for *E93* primers. The majority of reaction from 50 °C to 56 °C produced PCR products with faint gel bands. Reactions above 57 °C also showed bright bands. The temperature 60 °C was determined to be the optimal annealing temperature for *E93* primers. Reactions at 48 °C and 49 °C also showed bright bands, but these temperatures were not selected in order to reduce nonspecific primer bindings. Primers for the gene *E93* were further optimized for PCR conditions by performing PCR reactions on various concentrations of primers (Figure 10b). Initial primers concentration ranged from 50 nM to 200 nM. Reactions using

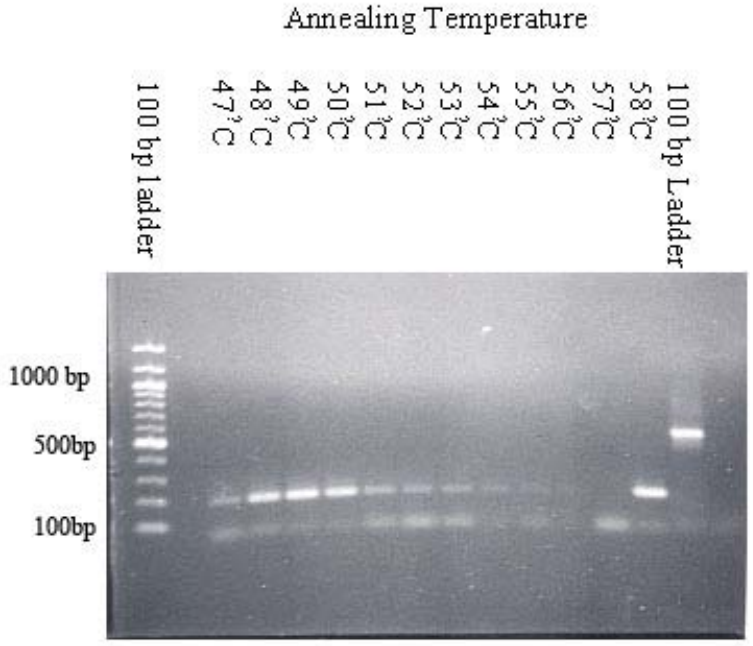

Figure 10a. *E93* primers annealing temperature optimization. Result suggested that 60 °C was the optimal annealing temperature for PCR conditions. PCR reactions performed at above this temperature produced PCR product with faint gel bands.

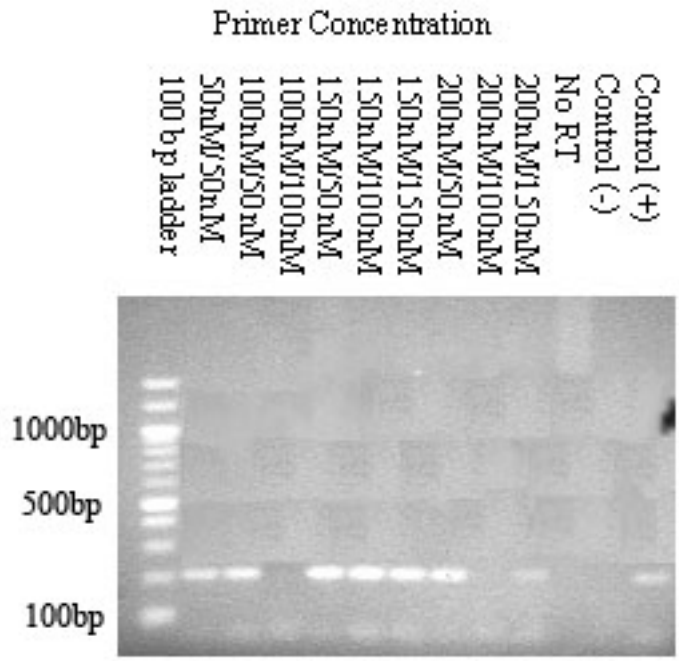

Figure 10b. *E93* primers concentration optimization. Result showed that primer concentration of 50 nM to 200 nM showed PCR product bands. The brightest bands were associated with primer concentration above 100 nM. The primer concentration of 200 nM was selected as the optimal primer concentration.

primer concentrations of 50 nM to 200 nM showed expected PCR product bands. The brightest bands were associated with primer concentration above 100 nM. However, at concentration 100 nM/100 nM, no band was present. This may have been the result of human error. The primer concentration of 200 nM was selected as the optimal primer concentration. This concentration complied with real-time PCR protocols. *β-actin* primers were optimized by Chisanga Lwatula.

Complementary DNA (cDNA) synthesis:

cDNA was produced using protocols from Invitrogen™. cDNA were made from total mRNA from control and experimental animals for 10 hrs and 12 hrs APF. No RT, positive control and negative control cDNA samples were produced to ensure cDNA was produced properly. Presence of PCR products from the no RT control would indicate that Superscript II Reverse Transcriptase was not necessary for the production of the PCR products in this reaction. Control cDNAs results were subjected to electrophosises along with the primer optimization trials (figure 7b). No product was observed for the no RT reaction and negative control.

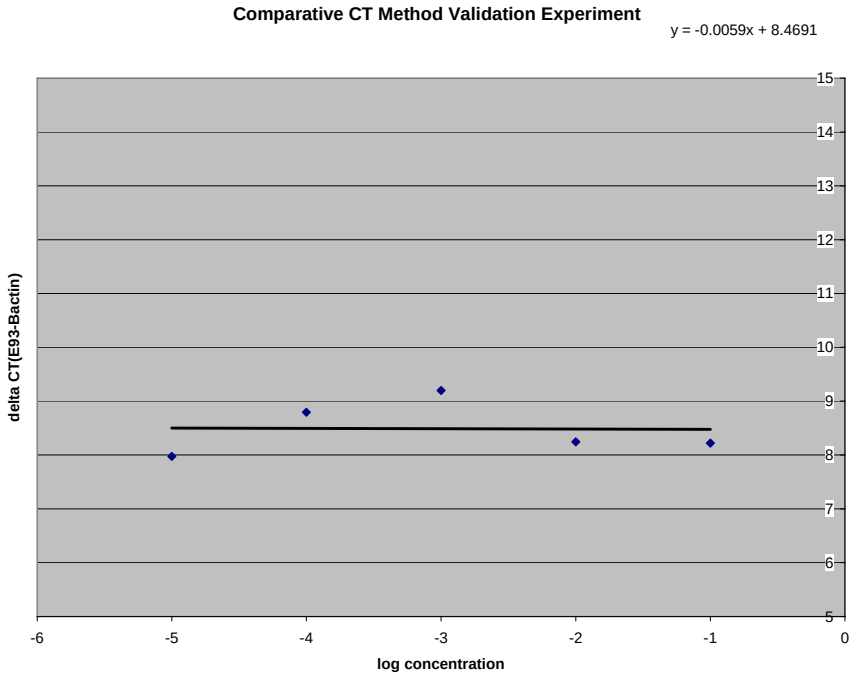

Figure 11. Validation of comparative C_T method. The use of the comparative C_T method was validated by performing a validation experiment. Observation of how ΔC_T varies with template dilution was performed. ΔC_T values were obtained from real-time PCR reactions and were plotted against log input. A slope of roughly zero would validate the use of the $\Delta\Delta C_T$ quantification method. Validation experiment produced a slope of -0.0059.

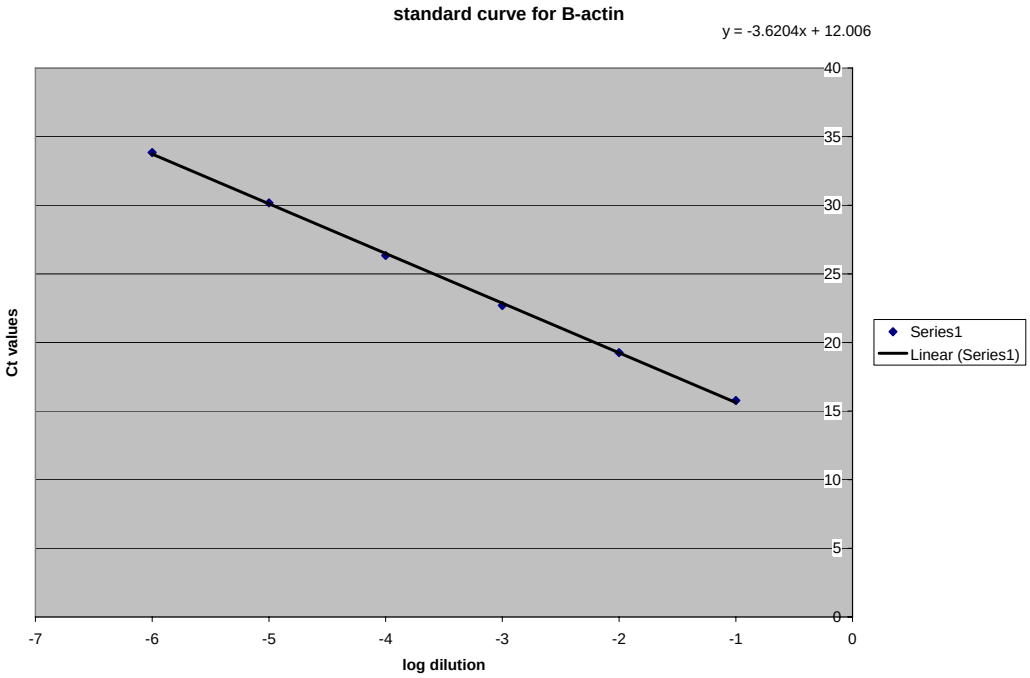

Figure 12. Standard curve for *β-actin* primer set. PCR amplification efficiency for the *β-actin* primer set was determined by performing real-time PCR reaction using *β-actin* primers on various dilution of mRNA input. C_T values of each reaction was determined and plotted against the log of input. In theory, a slope of -3.32 would indicate PCR amplification efficiency of 100%. *β-actin* standard curve produced a slope of -3.62 which suggests that PCR amplification using *β-actin* is highly efficient.

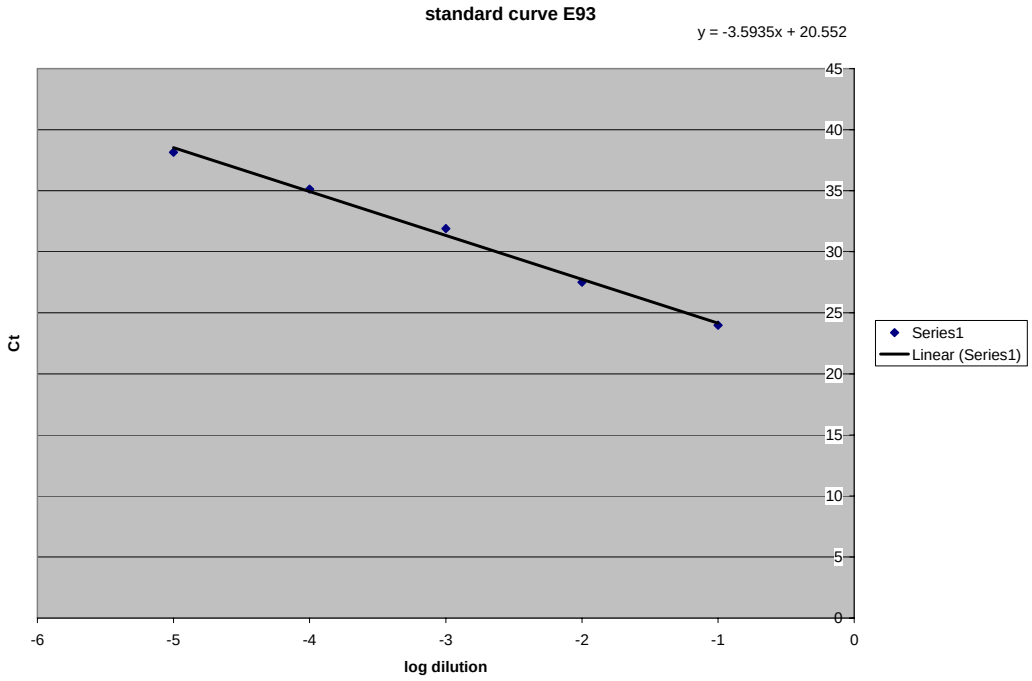

Figure 13. Standard curve for the *E93* primer set. A slope of -3.59 was calculated, suggesting that PCR amplification of *E93* is highly efficient.

Comparative C_T ($\Delta\Delta C_T$) analyses validation test:

The use of the comparative C_T method was validated by observing how ΔC_T varies with template dilution. ΔC_T values were obtained from real-time PCR reactions and were plotted against log input (Figure 11). A slope of -0.0059 was obtained. This suggests that with various mRNA concentration input, roughly the same level of expression was observed, after the reference was used to normalize the result. And that an error in mRNA input will skew the data. The small slope value validates the use of the $\Delta\Delta C_T$ quantification method.

PCR amplification efficiency test:

PCR amplification efficiency for *E93* and *B-actin* primer sets were determined by performing a standard curve. PCR reactions were performed on various dilutions of whole animal mRNA input. C_T values of each reaction was determined and plotted against log of input. A slope of -3.32 would indicate a 100% efficiency PCR reaction. A slope of -3.62 was obtained for the *β-actin* primer set (Figure 12), and a slope of -3.59 was obtained for the *E93* primer set (Figure 13).

Real-time PCR results:

Salivary Glands:

The comparative C_T ($\Delta\Delta C_T$) analyses of relative real-time PCR results suggest that there was an 8.09 fold underexpression of the gene *E93* at 10 hrs

APF in salivary glands tissues (Figure 14). An underexpression indicates that the gene *E93* was expressed less in *FTZ-F1*^{17}*/ Df(3L)Cat*^{DH104}salivary glands than in w^{1118} salivary glands. An overexpression would suggest that there was more expression of the gene *E93* in *FTZ-F1*^{17}*/ Df(3L)Cat*^{DH104} tissues than in w^{1118} tissues. 12 hrs APF results showed a 1.34 fold underexpression of *E93.* Note that two previous trials showed no expression of *E93* in 12 hrs APF mutant salivary glands. Standard deviation fold changes of 1.45 and 2.06 were observed for 10 hrs APF salivary glands and 12 hrs APF salivary glands, respectively (Table 4). A large standard deviation of fold change for 12 hrs APF tissues suggests that the observed underexpression of *E93* for 12 hrs APF salivary gland tissues is not significant.

Hindgut:

$\Delta\Delta C_T$ analyses showed similar *E93* expression patterns in hindgut tissues as salivary glands tissue of *βFTZ-F1* mutants. A 7.46 fold underexpression of *E93* in mutant 10 hrs APF hindgut tissues (Figure 15) and a standard deviation of 1.32 fold change was observed. Mutant 12 hrs APF hindgut tissues showed a 1.15 fold underexpression of *E93* and a standard deviation of 1.12 fold change (Table 5). A standard deviation of 1.11 fold change in mutant 12 hrs APF indicates that the slight underexpression of *E93* in mutant 12 hrs APF hindgut tissue is not significant.

Midgut:

βFTZ-F1 mutant's midgut tissues at both 10 and 12 hrs APF showed slight over expressions of *E93* at 1.05 fold and 1.80 fold, respectively (Figure

16). A standard deviation of 2.89 and 1.68 fold changes were observed for 10 hrs and 12 hrs APF tissues, respectively (Table 6). These relatively large standard deviations suggest that at both time points, *E93* is expressed at similar level in *βFTZ-F1* mutants as in control animals.

Fat body:

βFTZ-F1 mutant fat tissues showed a slight underexpression of *E93* (2.74 folds) at 10 hrs APF (Figure 17). A slight overexpression of *E93* (2.43 folds) was observed at 12 hrs APF in fat tissues. Standard deviation fold changes of 1.19 and 1.53 were calculated for 10 hrs APF and 12 hrs APF samples, respectively. Underexpression of *E93* in 10 hrs APF *βFTZ-F1* mutant fat body suggests that the expression of *E93* is not dependent on *βFTZ-F1* in this tissue at this time point. Large standard deviation fold change (Table 7) for 12 hrs APF fat body suggests that this slight underexpressions was not significant and that at this time point, *E93* was expressed in similar levels in both mutant and control animals.

Statistical Analysis:

T-tests were performed to assess whether results from the comparative C_T method were statistically significant (Table 3). A p-value of less than 0.05 would indicate that the result is significant. Results of T-tests support the experimental observations: data for 10 hrs APF salivary glands, 12hrs APF hindgut, and 10 hrs APF fat are significant.

Table 3. T-test assessment of results from the comparative C_T method. A p-value of less than 0.05 indicates that the result is significant.

	CT	Standard Error	P-value	Significant?
SG 10 hr	3.257	0.702704	0.043532	Yes
SG 12 hr	0.458	1.159881	0.731072	No
HG 10 hr	3.131	0.527126	0.027193	Yes
HG 12 hr	0.214	0.53477	0.727726	No
Fat 10 hr	1.574	0.397559	0.010752	Yes
Fat 12 hr	1.385	1.082715	0.236683	No
MG 10 hr	0.07	1.803884	0.969997	No
MG 12 hr	0.915	1.126307	0.440071	No

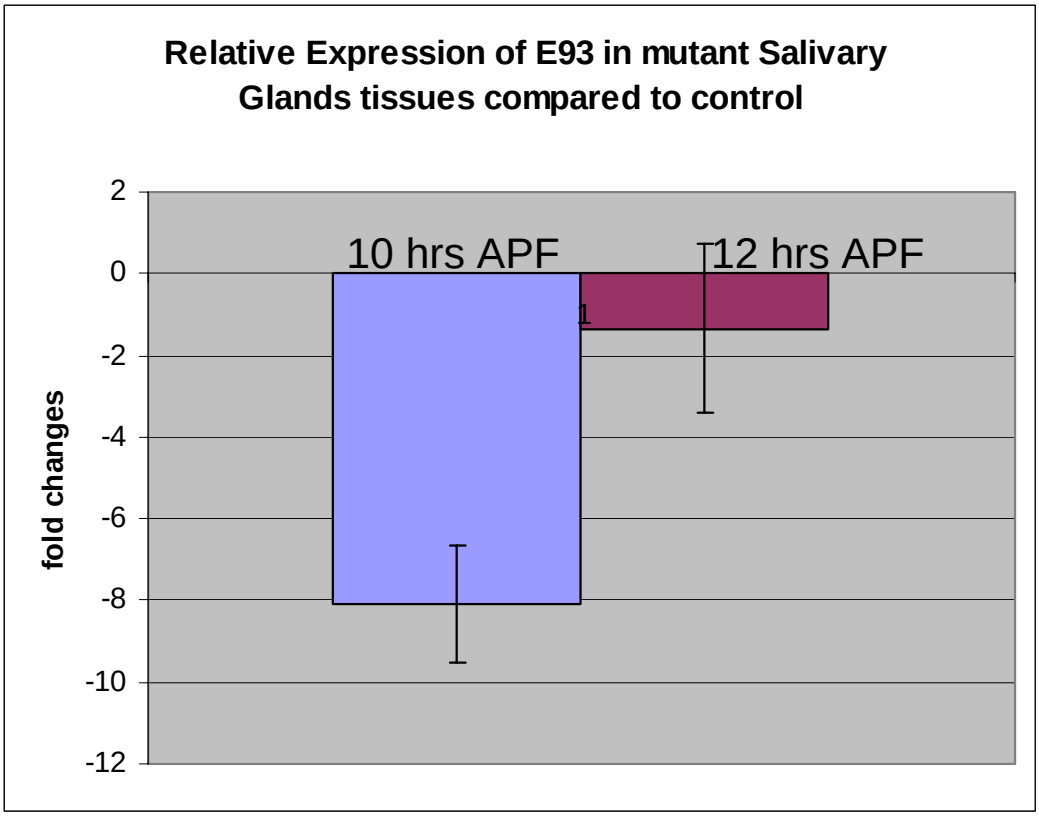

Figure 14. Expression of *E93* in *βFTZ-F1* mutant salivary glands. Comparative C_T ($\Delta\Delta C_T$) analyses of relative real-time PCR results show an 8.09 fold underexpression of the gene *E93* in mutant 10 hrs APF salivary glands. A 1.34 fold underexpression of *E93* was observed in mutant 12 hrs APF salivary glands. A large fold change standard deviation for 12 hrs APF tissues suggests that the observed underexpression was not significant.

Table 4. Fold change of *E93* expression in *βFTZ-F1* mutant salivary glands compared to control salivary glands. Comparative C_T ($\Delta\Delta C_T$) analyses of relative real-time PCR results for salivary gland tissues show 8.09 underexpression of *E93* in 10 hrs APF tissues with a standard deviation of 1.45 fold change. 12 hrs APF salivary glands results show a slight underexpression of 1.34 fold with a standard deviation of 2.06 fold.

Time	Fold change	Standard deviation of the fold change
10 hrs APF	-8.09	1.45
12 hrs APF	-1.34	2.06

Table 5. Fold change of *E93* expression in *βFTZ-F1* mutant hindgut compared to control hindgut. $\Delta\Delta C_T$ analyses showed an underexpression of *E93* in 10 hrs APF hindgut tissues of *βFTZ-F1* mutants. A slight underexpression of *E93* in 12 hrs APF hindgut tissues was observed. Standard deviation of 1.32 fold change and 1.12 fold change were observed in 10 hrs APF hindgut and 12 hrs APF hindgut, respectively.

Time	Fold change	Standard deviation of the fold change
10 hrs APF	-7.46	1.32
12 hrs APF	-1.15	1.12

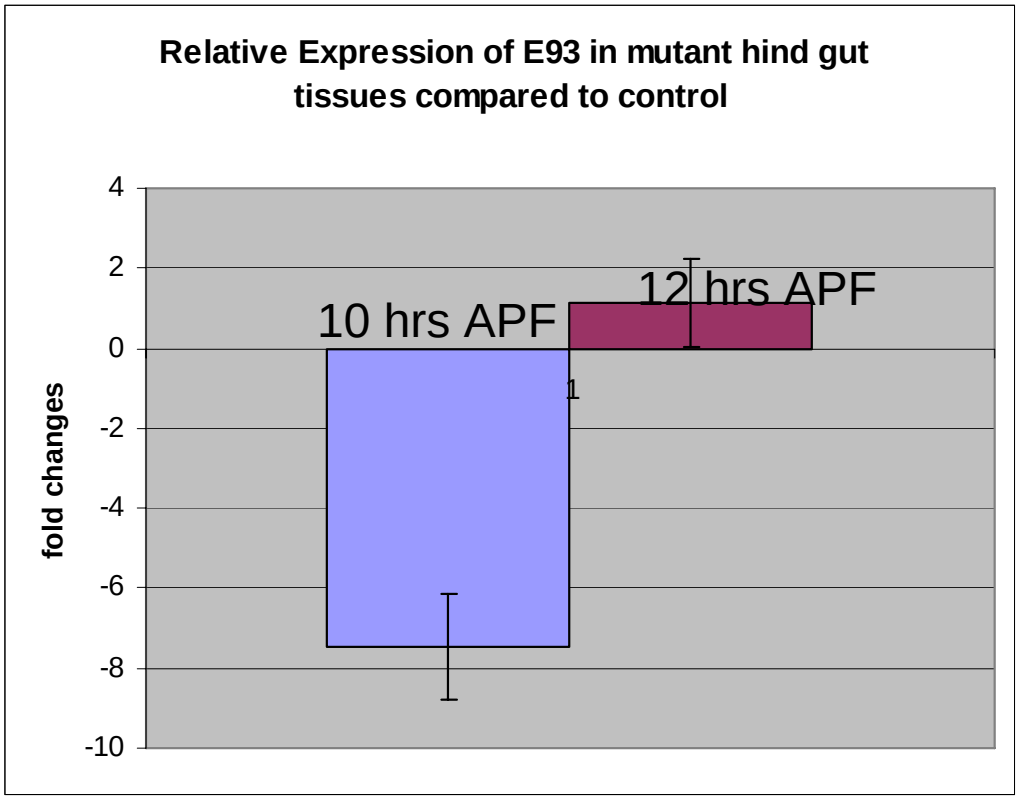

Figure 15. Expression of *E93* in *βFTZ-F1* mutant hindgut. $\Delta\Delta C_T$ analyses showed a 7.46 folds underexpression of *E93* in mutant hindgut tissues and a slight underexpression of *E93* in 12 hrs APF hindgut. The large fold change standard deviation for 12 hrs APF tissues suggests that the underexpression of *E93* in this tissue is not significant.

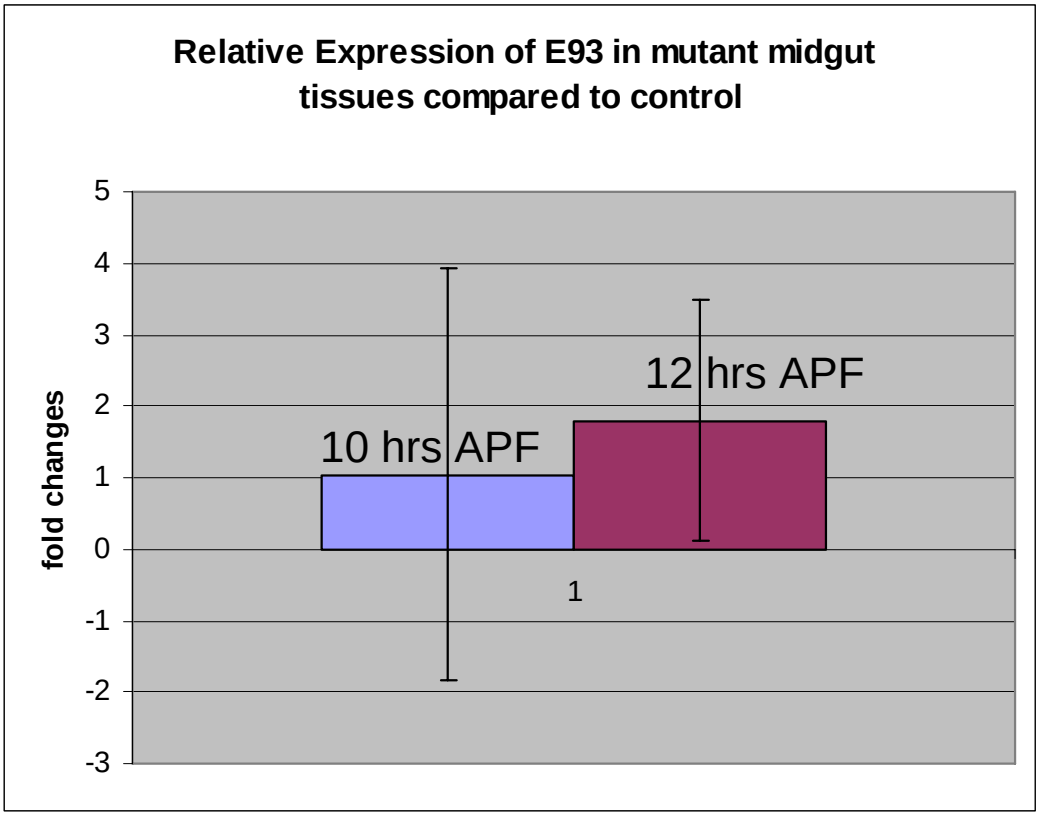

Figure 16. $\Delta\Delta C_T$ analyses showed a slight overexpression of *E93* in both 10 hrs APF and 12 hrs APF midgut tissues of *βFTZ-F1* mutants, respectively. Standard deviation fold changes for these expression are relatively high, thus, the observed overexpression is not significant.

Table 6. Fold change of *E93* expression in *βFTZ-F1* mutant midgut compared to control midgut. A slight overexpression of *E93* were observed in both 10 and 12 hrs APF midgut tissues of *βFTZ-F1*mutants. Relatively large stand deviation fold changes suggest that similar levels of *E93* expression were observed in both mutant and control animals at these time points.

Time	Fold change	Standard deviation of the fold change
10 hrs APF	1.05	2.87
12 hrs APF	1.80	1.68

Table 7. Fold change of *E93* expression in *βFTZ-F1* mutant fat body compared to control fat body. *βFTZ-F1* mutant fat body showed a slight underexpression of *E93* at 10 hrs APF (2.74 folds) and a slight overexpression at 12 hrs APF (2.43 folds). A standard deviation fold changes of 1.19 and 1.53 were observed for 10hrs APF and 12 hrs APF.

Time	Fold change	Standard deviation of the fold change
10 hrs APF	-2.74	1.19
12 hrs APF	2.43	1.53

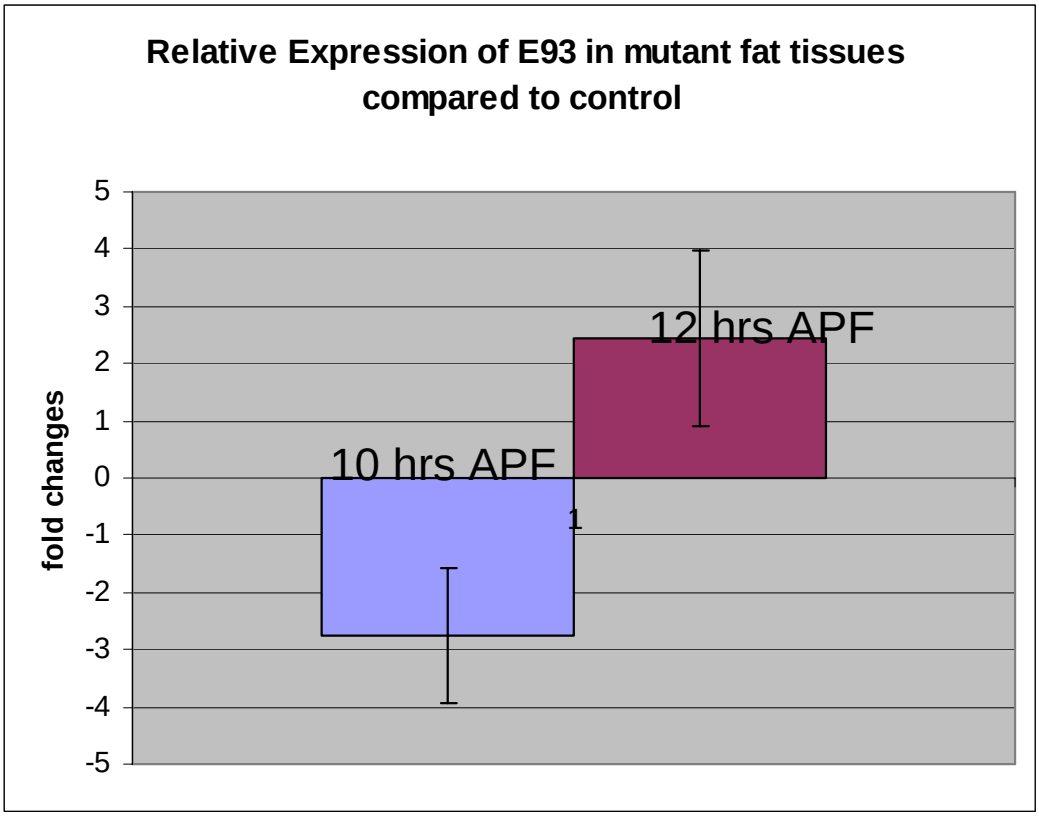

Figure 17. An underexpression of *E93* was observed (2.74 folds) in 10 hrs APF fat tissues of *βFTZ-F1*mutant. A slight overexpression of *E93* was observed (2.43 folds) for 12 hrs APF fat tissues. Relatively large standard deviation fold change was observed for *E93* expressions in 12hrs APF fat body tissues, suggesting that this expression is not significant.

DISCUSSION

Primer optimizations:

Real-time PCR were performed at *E93* primers' optimal annealing temperature (60°C) and concentration (200 nM). Though optimization results suggested that most PCR reactions performed on an annealing temperature gradient of 47°C to 60°C produced the expected PCR product, the highest temperature was selected. Because cDNAs libraries contain thousands of genes, non-specific amplification of an unwanted gene may be produced with PCR. To avoid non-specific primer extension by DNA polymerase, a higher annealing temperature was selected to reduce non-specific primer annealing.

The majority of PCR reactions with varying primer concentrations from 50 nM to 200 nM produced expected PCR product. However, the reaction containing primer concentrations of 100 nM produced no product. Because reactions using both less and more primer concentrations yielded products, the result of this reaction may be due to human errors. Perhaps reagents were not properly combined or pippetting deviation s may have occurred.

Real-time PCR data:

A validation experiment for the comparative C_T method was performed. A plot of ΔC_T vs. log of input yielded a slope of -0.0059. The

efficiency of *E93* and *β-actin* must approximately equal (<0.1) to pass the validation test for the $\Delta\Delta C_T$ method. Thus, a slope of -0.0059 indicated that the $\Delta\Delta C_T$ could be use to analyze real-time PCR data.

$\Delta\Delta C_T$ analyses of salivary glands showed an underexpression of *E93* in 10 hrs APF tissues of *βFTZ-F1* mutants. This means that the mutant salivary glands expressed less *E93* than salivary glands of control animals. These mutants had one poorly functioning copy of the *βFTZ-F1* gene. In control salivary glands, *βFTZ-F1* functions as a competence factor for the reinduction of a set of early genes in response to the prepupal pulse of ecdysone (Woodard *et al*., 1994). Thus, an underexpression of *E93* would suggest that the gene *βFTZ-F1* was necessary for the expression of *E93* in this tissue.

Experimental data suggesting that the expression of *E93* was dependent of *βFTZ-F1* in 10 hrs APF salivary glands is supported by previous genetic studies. Ectopic expression of *βFTZ-F1* transgene in late third instar larvae was sufficient to activate transcription of the pupal-specific *E93* early gene (Woodard *et al.,* 1994). The *E93* gene appears to be a regulator of cell death (Lee and Baehrecke, 2001), and *E93* mutants have defects in larval salivary gland cell destruction. In studies by Lee and colleagues (2002), it was observed that *E93* was required for premature death of salivary glands induced by ectopic expression of *βFTZ-F1.* Also, *βFTZ-F1* was required for DNA fragmentation during salivary gland programmed cell death (Lee *et al.,* 2002).

In control animals, *E93* is expressed during the prepupal pulse of ecdysone; and the salivary glands undergo programmed cell death by ~15 hours APF in response to this ecdysone pulse (Robertson, 1936). In control salivary gland, the presence of *βFTZ-F1* enables *E93* to respond to the pre-pupal pulse of ecdysone, resulting in cell death in this tissue. In contrast, in *βFTZ-F1* mutant salivary gland, *E93* could not be induced by ecdysone in the absence of *βFTZ-F1.* Thus, an underexpression of *E93* was expected.

E93 was expected to not respond to the prepual pulse of ecdysone in the absence of *βFTZ-F1* in salivary glands, and thus, an underexpression of *E93* was expected and observed at 10 hr APF. However, 12 hrs APF *βFTZ-F1* mutant salivary gland tissues showed a slight underexpression of *E93*, accompanied by a large fold change standard deviation. The large standard deviation indicates that the underexpression was not significant, and that both *βFTZ-F1* mutant salivary gland and control animals expressed similar levels of *E93* mRNA at this time. Reasons for the slight underexpression of *E93* in 12 hrs APF *βFTZ-F1* mutant salivary gland are unclear. However, this observation may be a result of human errors or insufficient trials. Or perhaps a delay of *E93* expression was observed in *βFTZ-F1*mutant salivary gland, in that a reduced expression of *E93* was observed at 10 hrs APF but two hours later, normal level expression was observed. *βFTZ-F1* mutants had one poorly functioning copy of the gene *βFTZ-F1.* In mutants with *βFTZ-F1* completely removed at these time points, an underexpression of *E93* is expected. In this study, *βFTZ-F1* mutants expressed a reduced level of full length *βFTZ-F1*

transcript and may elicit a delayed response. Thus, expression of *E93* was observed at a later time point.

A similar *E93* expression pattern was observed for hindgut tissues as salivary gland tissues of *βFTZ-F1*mutants. 10 hrs APF mutant hindgut tissues showed an underexpression of *E93.* An underexpression of *E93* in 10 hrs APF means that mutant hindgut expressed less *E93* than control hindgut, suggesting that *βFTZ-F1* was necessary for the expression of *E93.* A not significant underexpression of *E93* was observed at 12 hrs APF *βFTZ-F1* mutant hindgut tissues. Reasons for this underexpression of *E93* are unclear. 12 hrs APF data suggests that *βFTZ-F1* was not required for the expression of *E93.* Again, the increase in *E93* expression two hours following 10 hrs APF may suggest a delay in *E93* expression in *βFTZ-F1* mutant hindgut.

Hindgut, like salivary glands, undergoes cell death as a response to the prepupal pulse of ecdysone (Baehrecke, 2000). During this time, larval hindgut is replaced by the adult hindgut. Therefore, *E93* is expected to be expressed during the later stages of development, in synchrony with the prepupal pulse of ecdysone. Experimental data suggest that the expression of *E93* in hindgut at 10 hrs APF is dependent on *βFTZ-F1.* It is likely that *βFTZ-F1* also functions as a competence factor of *E93* to response to ecdysone in the hindgut.

If steroid genetic regulatory hierarchy in larval salivary glands applies to midgut and fat body, then it can be hypothesized that the expression of *E93*

is not dependent on *βFTZ-F1* in these tissues. *βFTZ-F1* is expressed during a period of low ecdysone concentration, after the larval pulse of ecdysone. Because *βFTZ-F1* is expressed after the initiation of programmed cell death in midgut and fat body, it was expected that *E93* expression should be observed in *βFTZ-F1* mutant midgut and fat body. Experimental data of 10 hrs APF and 12 hrs APF midgut tissues of *βFTZ-F1* mutants showed overexpression of *E93*. Large fold change standard deviations were observed for these time points. This means that the observed over expressions of *E93* were not significant, indicating that both *βFTZ-F1* mutants and control animals expressed similar level of *E93* transcript in midgut tissues at these time points. This suggests that *βFTZ-F1* was not necessary for the expression of *E93* in midgut tissues at 10 hrs APF and 12 hrs APF.

Experimental data suggest that the expression of *E93* is not dependent on *βFTZ-F1* in the midgut. This is supported by previous genetic studies. Unlike the salivary gland and hindgut which undergo cell death in response to the prepupal pulse of ecdysone, the larval midgut undergoes cell death at puparium formation (zero hr APF) in response to the late larval pulse of ecdysone (Jiange *et al.,* 1997). In newly formed prepupae, *E93* is expressed in the midgut. Continued expression *E93* was observed following the prepupal ecdysone pulse (Baehrecke and Thummel, 1995). Because the expression of *E93* occurs before the expression of *βFTZ-F1* in the midgut, it is likely that these gene works independently in this tissue.

Cell death of larval midgut differs from cell death of salivary glands. Ecdysone triggers midgut cell death at a stage when salivary glands synthesize and secrete polypeptide glue. Genetic studies have connected the destruction of larval salivary glands with the expression of *E93* and *βFTZ-F1*. However, *βFTZ-F1* is not expressed in midgut prior to this tissue's ecdysone-induced expression of *E93* and cell death. In this study, midgut data suggested that *βFTZ-F1* was not necessary to provide *E93* with the competence to respond to ecdysone in this tissue. Lee and colleagues (2002) hypothesized that midgut cell death is a result of ecdysone receptor complex activating *BR-C* and *E93* independently of *βFTZ-F1* or that another unrelated transcription regulator may regulate these early genes. Their study showed that larval midgut destruction occurs via autophagy. They observed that mutations in the *E93* gene prevented destruction of midgut cells, but also possess fragmented DNA. The gene *E93* appeared to influence ecdysone induction of cell death during metamorphosis, but also appeared to require other regulatory factors to properly activate the programmed cell death response (Baehrecke, 2000). In addition, *E93* is expressed in the midgut at zero hours APF (Baehrecke and Thummel, 1995) while *βFTZ-F1* is not induced in the midgut until 6-8 hr after *E93* is induced. Thus, the regulation of *E93* may not depend on *βFTZ-F1* in the midgut and may rely on another unidentified factor(s) (Li and White, 2003).

Experimental data of 10 hrs APF *βFTZ-F1* mutant fat body showed an underexpression of *E93*. Here, the expression of *E93* appears to be

dependent on *βFTZ-F1*. However, 12 hrs APF fat body showed a slight overexpression of *E93*. T-test result for this time point suggests that the slight overexpression is insignificant, indicating that both *βFTZ-F1*mutant and control animal expressed similar level of *E93* in fat body at 12 hrs APF. This suggests that *βFTZ-F1* is necessary for the expression of *E93* at 10 hrs APF, but is not necessary for the expression of *E93* in fat body at 12 hrs APF.

The expression pattern of *E93* in midgut is similar to the expression of *E93* in fat body. Low level of *E93* was detected in fat body in newly formed prepupae. This level of *E93* expression increased in fat body of late prepupae as a response to the prepupal pulse of ecdysone (Baehrecke and Thummel, 1995). The decreased level of *E93* expression in 10 hrs APF fat body may be a result of a delay expression of *E93* due to the hypomorphic characteristic of the experimental animals. When enough *βFTZ-F1* transcripts have accumulated, the level of *E93* expression would increase. The increased level of *E93* expression was observed in 12 hrs APF fat body.

Literature data suggests that expression of *E93* in fat body of newly formed prepupae may be *βFTZ-F1* independent in that *βFTZ-F1* does not function as the competence factor for *E93* expression in this tissue. However, results of this study suggest that the expression of *E93,* as a response to the prepupal pulse of ecdysone, may be enhanced by *βFTZ-F1*.

Metamorphosis of *Drosophila melanogaster* involves the destruction of most of the larval tissues. During the transition from the third instar to a

prepupa, many tissues undergo metamorphic changes in synchrony with the rise of the late larval ecdysone titer. For example, larval midguts are destroyed (Robertson, 1936). Likewise, the transition of the prepupal-to-pupal is accompanied with metamorphic changes. The larval salivary glands undergo programmed cell death while adult salivary glands initiate morphogenesis (Robertson, 1936).

The destruction of larval tissue is necessary for proper development. Steroid hormones appear to regulate programmed cell death by regulating the relationship between *βFTZ-F1* and *E93.* For example*,* the destruction of fat body and midgut tissues initiate at puparium formation with the expression of *E93.* The proper timing of this event is regulated by having the expression of *E93* in these tissues not dependent on *βFTZ-F1,* which is expressed later during the mid-prepupal stage. However, the salivary gland and hindgut undergo programmed cell death much later in development. The expression of *E93* in these tissues is dependent on *βFTZ-F1.* Therefore, expression of *E93* cannot initiate without the presence *βFTZ-F1* in these tissues. Thus, the fly is able to regulate the timely destruction of larval tissues by controlling the expression of *E93* through *βFTZ-F1.* This control mechanism is supported by the results of this study.

Future directions:

Larval tissues undergo cell death during *Drosophila* metamorphosis in a stage-specific manner. In this studies, data suggested that the gene *βFTZ-F1*

is not required for the expression of the gene *E93* in both fat and midgut tissues. In contrast, *βFTZ-F1* is required for the expression of *E93* in 10hrs APF salivary glands and hindgut tissues. To further this study, additional real-time PCR trials must be performed. Data for fat and midgut tissues were compiled from three trials with each trial containing three replicated reactions, totaling to nine reactions for each tissue sample. Also, additional data should be collected for salivary gland and hindgut tissues. Current data for these tissues were based on three reactions. Six reactions were previously preformed for salivary glands but the data from these trials could not be incorporated into the data analysis due to complication with the comparative C_T analysis protocol. The numbers of reaction should be increased for result accuracy.

In addition to increasing the number of reaction, the study can be bettered by extending the experiment to include other tissues (CNS and imaginal discs) and other early genes (*BR-C, E74A, E75A)*. Extending this study to include other early gene may provide more details on hierarchy of ecdysone actions in *Drosophila* metamorphosis. It was observed that early genes (*BR-C, E74, E75)* and cell death genes (*rpr, hid, crq,* and *dronc)* are all transcribed at reduced levels in *E93* mutant salivary glands*(*Lee *et al*., 2000). And that the expression of *E93* was dependent on *BR-C* (Baehrecke *et al.,* 1995). These early genes were thought to influence the transcription of programmed cell death genes prior to the larval salivary gland death (Jiang *et al.*, 2000). Also, *E74A* transcription in the salivary glands parallels that of *E93.*

It would be interesting to see if *βFTZ-F1* shares a similar relationship with *E74A* as it does with *E93* in selected tissues.

Furthering this study to include CNS and imaginal discs may reveal similar *βFTZ-F1* relationship in these tissues in that *βFTZ-F1* provides *E93* with the competence to respond to ecdysone in these tissues. CNS and imaginal disc have similar *E93* expression pattern. Baehrecke and Thummel study (1995) showed that *E93* transcript accumulated in a stage-specific manner in the CNS and imaginal discs of late prepupae, following the prepupal ecdysteroid pulse.

REFERENCES

Ashburner, M. 1972. Puffing patterns in *Drosophila melanogaster* and related species. *Results and Problems in Cell differentitation.* 4: 101-151 (Ed. W. Beermann). Berlin: Springer-Verlag.

Ashburner, M. 1973. Sequential gene activation by ecdysone in polytene chromosomes of *Drosophila melanogaster.* I. Dependence upon ecdysone concentration. *Dev. Biol.* 35, 47-61.

Aranda, A. and Pascaul, A. 2001. Nuclear hormone receptors and gene expression. *Pys. Reviews* 81(3), 269-1304.

Baehrecke, E.H. and Thummel, C.S. 1995. The *Drosophila E93* Gene from the 93F Early Puff Displays Stage- and Tissue-Specific Regulation by 20-Hydroxyecdysone. *Developmental Biology* 171, 85-97.

Baehrecke, E. H. 2000. Steroid regulation of programmed cell death during Drosophila Development. *Cell Death Differ.* 7, 1057-1062.

Bodenstein, D. 1965. The post-embryonic development of *Drosophila.* In *Biology of Drosophila (*M. Demerec, ed.). New York: Hafner Publishing Co., pp. 275-367.

Broadus, J.; McCabe, J.; Endrizzi, B.; Woodard, C.; 1999. Drosophila BFTZ-F1Orphan Nuclear Receptor Provides Competence for Stage-Specific Responses to the Steroid Hormone Ecdysone. *Molecular Cell* 3, 143-149.

Alberts, B., Johnson, A., Lewis, J., Raff, M., Roberts, K., and Walter, P. 2002. Molecular Biology of the Cell. 4th ed. New York: Garland Publishing.

Burtis, K.C., Thummel, C.S., Jones, C.W., Karim, F.D., and Hogness, D.S. 1990. The *Drosophila* 74EF early puff contains *E74*, a complex ecdysone-induced gene that encodes two ets-related protein*s. Cell* 61, 85-99.

Cheng-Yu L., Cooksey B.A.K, and Baehrecke E.H. 2002. Steroid regulation of midgut cell death during *Drosophila* development. *Developmental Biology* 205, 101-111.

DiBello, P.R., D.A. Wither, C.A. Bayer, J.W. Fristrom, and G.M. Guild. 1991. The *Drosophila* Broad Complex encodes a family of related proteins containing zinc fingers. *Genetics* 12, 385-397.

Fletcher, J.C., Thummel, C.S . 1995. The ecdysone-inducible Broad-complex and E74 early genes interact to regulate target gene transcription and Drosophila metamorphosis. *Genetic* 141, 1025-1035.

Forman, D.M and Samuels H.H. 1990. Dimerization among nuclear hormone receptors. *New Biol.* 2(7), 587-94.

Foye, W.O, Lemke, T.L., Williams, D.A. Principles of Medicinal Chemistry. Fourth Edition. Williams & Wilkins, 1995.

Guichet, A., Copeland, J.W.R., Erdelyl, M., Hlousek, D., Zavorszky, P., Ho, J., Brown, S., Percival-Smith, A., Krause, H.M., Ephrussi,A. 1997. The nuclear receptor homologue *FTZ-F1* and the homeodomain protein Ftz are mutually dependent cofactors. *Nature* 385, 548-552.

Heftmann, E., Mosetting, E. 1960. *Biochemistry of steroids.* Reinhold Publishing Corp., NY.

Horner, M.A., Chen, t. And Thummel, C.S. 1995. Ecdysteroid regulation and Dna binding properties of *Drosophila* nuclear hormone receptor superfamily members. *Developmental Biology* 168, 490-502.

Huet, F., Puiz, C. and Richards G. 1993. Puffs and PCR: the in *vivo* dynamics of early gene expression during ecdysone responses in *Drosophila*. *Development* 118, 613-627.

Jiang, C., Baehrecke, E.H., and Thummel, C.S 1997. Steroid regulated programmed cell death during *Drosophila* metamorphosis. *Development* 124, 4673-1683.

Jiang C, Lamblin A-FJ, Steller H and Thummel CT. 2000. A steroid-triggered transcriptional hierarchy controls salivary gland cell death during *Drosophila* metamorphosis. *Mol. Cell.* 5, 445-455.

Jochova J., Zakeri Z., Lockshin RA. (1997) Rearrangement of the tubulin and actin acytoskelteon during programmed cell death in *Drosophila* salivary glands. *Cell Death Diifer.* 4, 140-149.

Karim, F.D., Guild, G.M. and Thummel, C.S. 1993. The *Drosophila Broad-Complex* plays a key role in controlling ecdysone-regulated gene expression at the onset of metamorphosis. *Development* 118, 977-988.

Kiss, I., A.H. Beaton, J. Tardiff, D. Fristrom, and J.W. Fristrom. 1988. Interactions and developmental effects of mutations in the Broad-Complex in *Drosophila melanogaster*. *Genetics* 18, 247-259.

Koelle, M. R., Talbot, W.S., Segraves, W.A., Bender, M.T, Cherbas, P., and Hogness, D.S. 1991. The *Drosophila* EcR gene encodes an ecdysone receptor, a new member of the steroid receptor superfamily. *Cell* 67. 59-77.

Koelle M.R. Segraves W.A, Hogness D.S. DHR3: a Drosophila steroid receptor homolog. *Proc Natl Aca Sci.* 89(13), 6167-71.

Lavorgna, F., Karim, F.D., Thummel, C.S., Wu, C. 1993. the Potential role for a *FTZ-F1* steroid receptor superfamily member in the control of *Drosophila* metamorphosis. *Proc. Natl. Acad. Sci USA* 90, 3004-3008.

Lee C.Y., Wendel D.P., Reid P., Lam G., Thummel C.S., and Baehrecke E.H. 2000. *E93* directs steroid-triggered programmed cell death in *Drosophila. Mol Cell* 6, 433-443.

Lee, C.Y. and Baehrecke, E.H. 2001. Steroid regulation of autophagic programmed cell death during development. *Development* 128, 1443-1455.

Lee, C.Y.; Simon, C.; Woodard C.; Baehrecke, E.; 2002. Genetic Mechanism for the Stage – and Tissue Specific Regulation of Steroid Triggered Programmed Cell Death in Drosophila. *Dev. Biol.* 252,138-148.

Levis, R., Hazelrigg, T., and Rubin G. 1993. Separable cis-acting control elements for expression of the *white* gene of *Drosophila. EMBO.* 4, 3489-3499.

Lockshin, R.A., and Zakeri, Z. 1991. Programmed cell death and apoptosis. In "Apoptosis: The Molecular Basis of Cell Death." (L.D. Tomei and F.O. Cope, Eds.), Vol. 3, pp 47-60. Cold Spring Harbor Laboratory Press, Cold Spring Harborm NY.

Mangelsdorf, D.J., Evans, R.M. 1995. The RXR heterodimers and orphan receptors. *Cell* 83, 935-839.

Messer, W.S. 2000. "MBC 3320 Steroid hormones and receptors." Home page: http://www.neurosci.pharm.utoledo.edu/MBC3320/steroids.htm.

Mlodzik M., Hiromi Y., Weber U., Goodman C.S., Rubin G.M. 1990. The Drosophila seven-up gene, a member of the steroid receptor gene superfamily, controls photoreceptor cell fates. *Cell* 60(2):211-24.

Oro A.E., McKeown M., Evans R.M. 1990. Relationship between the product of the Drosophila ultraspiracle locus and the vertebrate retinoid X receptor. *Nature* 347(6290), 298-301.

Pignoni, F., Baldarlli, R.M, Steingrimsson, F., Diaz, R.J., Patapoutian A., Merriam J.R., Lengyel J.A. 1990. *Cell* 62(1), 151-63.

Restifo L.L. and K. White. 1992. Mutations in a steroid hormone-regulated gene disrupt the metamorphosis of internal tissues in *Drosophila*. *Dev. Biol.* 20, 221-234.

Richards, G. 1976. Sequential gene activiation by ecdysone in polytene chromosome of *Drosophilia melanogaster.* IV. The mid prepupal period. *Dev. Biol.* 54, 256-263.

Richards, G. 1981. The radioimmune assay of ecdysteroid titers in *Drosophila melanogaster. Mol. Cell Endocrinol.* 21,181-197.

Riddiford, L. M.1993. "Hormones and *Drosophila* Development"- in *The development of Drosophila melanogaster*. ed. M. Bate and A Martinez Arias. Cold Spring Harbor Laboratory Press. Cold Spring Harbor, pp 899-939.

Robertson, C.W. 1936. The metamorphosis of *Drosophila* CNS is ecdysone-regulated and coupled with a specific ecdysone receptor isoform. *Development* 119, 1251-1259.

Schweichel, J.U., and Merker, H.J. 1973. The morphology of various types of cell death in prenatal tissues. *Teratology* 7, 253-266.

Segraves, W.A. 1998. Molecular and genetic analysis of the *E75* ecdysone-responsive gene of *Drosophila melanogaster*. Pd.D. thesis, Stanford University.

Seagraves W. A. and D. S Hogness 1990. The E75 ecdysone-inducible gene for the 75B early puff in *Drosophila* encodes two new members of the steroid receptor superfamily. *Genes Dev*. 4, 204-219.

Talbot W.S., Swyryd, E.A. and Hogness, D.S. 1993. *Drosophila* tissues with different metamorphic responses to ecdysone express different ecdysone receptor isoforms. *Cell* 73(7), 1323-37.

Thummel, C.S., Burtis, K.C, and hogness, D.S. (1990). Spatial and temporal patterns of *E74* transcription during Drosophila development. *Cell* 61, 101-111.

Thummel, C.S..1996. Flies on steroids – *Drosophila* metamorphosis and the mechanisms of steroid hormone action. *Trends in Genetics* 12, 306-310.

Thummel, C.S. 2001. Steroid-triggered death by autophagy. *BioEssays* 23, 677-682.

Urness, L.D. and Thummel, C.S. 1990. Molecular interactions within the ecdysone regulatory hierarchy: DNA binding properties of the *Drosophila* ecdysone-inducible *E74a* protein. *Cell* 60, 47-61.

[VCU] Virginia Commonwealth University. October 16, 2000. Home page: http://www.people.vcu.edu/~urdesai/estr.htm

Von Gaudecker, B. and Schmale EM. Substrate-histochemical investigations and ultrahistochemical demonstrations of acid phosphatase in larval and prepupal salivary glands of *Drosophila melanogaster. Cell Tissu Res.* 155, 75-89.

Von Kalm, L., Crossgrove, K., Von Seggern, D., Guild, G.M. and Beckendorf, S.K. 1994. The *Broad-Complex* directly controls a tissue-specific response to the steriod hormone ecdysone at the onset of *Drosophila* metamorphosis. *EMBO J.* 13, 3505-3516.

Woodard C.T., Baehrecke, E.H., and Thummel, C.S. 1994. A molecular mechanism for the stage-specificity of the *Drosophila* prepupal genetic response to ecdysone. *Cell* 79, 607-615.

Yamada, M., Murata, T., Hirose, S., Lavorgna, G., Suzuki, E., Ueda, H. 2000. Temporally restricted expression of transcription factor β*FTZ-F1*: significance for embryogenesis, molting and metamorphosis in *Drosophila melanogaster. Development* 127, 5083-5092.

Yamamoto, K.R. 1985. Steriod receptor regulated transcription of specific genes and gene networks. *Annu. Rev. Genet.* 19, 209-252.

APPENDIX

Robb's Solution:

100mL of Robb's solution =50mL solution + 5mL solution B + 45mL dH20.

Solution A (2X)

104 nM NaCl
80 nM KCl
20 nM glucose
0.2 M sucrose
2.4 nM $MgS0_4$. 7 H_2O
2.4 nM $MgCl_2$. 6 H_2O
2.4 nM $CaCl_2$. 2 H_2O

Solution B (20X)

40 nM Na_2HPO_4
7.4 nM KH_2PO_4
4 nM NaOH